The Hydrogen Isotope Composition δ^2H Reflects Plant Performance[1]

Rut Sanchez-Bragado,[a,2] Maria Dolors Serret,[a] Rosa Maria Marimon,[b] Jordi Bort,[a] and José Luis Araus[a,3,4]

[a]Secció de Fisiologia Vegetal, Facultat de Biologia, Universitat de Barcelona, Barcelona and AGROTECNIO (Centre for Research in Agrotechnology), Lleida, Spain 08028

[b]Unitat de Medi Ambient, Scientific and Technological Centers of the University of Barcelona, Barcelona, Spain 08028

ORCID IDs: 0000-0003-4236-549X (R.S.-B.); 0000-0003-4025-3929 (M.D.S.); 0000-0002-9264-0157 (J.B.); 0000-0002-8866-2388 (J.L.A.).

The stable carbon ($\delta^{13}C$) and oxygen ($\delta^{18}O$) isotope compositions in plant matter reflect photosynthetic and transpirative conditions in plants, respectively. However, the nature of hydrogen isotope composition (δ^2H) and what it reflects of plant performance is poorly understood. Using durum wheat (*Triticum turgidum* var *durum*), this study evaluated the effect of different water and nitrogen growing field conditions on transpiration and how this effect influenced the performance of δ^2H in autotrophic (flag leaf), mixotrophic (ears), and heterotrophic (grains and roots) organs. Moreover, δ^2H was compared with the $\delta^{13}C$ and $\delta^{18}O$ in the same organs. Isotope compositions were analyzed in dry matter, the water-soluble fraction, and in water from different tissues of a set of genotypes. Similar to $\delta^{13}C$, the δ^2H correlated negatively with stomatal conductance, whereas no correlation was observed for $\delta^{18}O$. Moreover, δ^2H was not only affected by changes in transpiration but also by photosynthetic reactions, probably as a consequence of NADPH formation in autotrophic organs. Compared with the δ^2H of stem water, plant δ^2H was strongly diminished in photosynthetic organs such as the flag leaves, whereas it strongly increased in heterotrophic organs such as grains and roots. In heterotrophic organs, δ^2H was associated with postphotosynthetic effects because there are several processes that lead to ^2H-enrichment of carbohydrates. In summary, δ^2H exhibited specific features that inform about the water conditions of the wheat crop, together with the photosynthetic characteristics of the plant part considered. Moreover, correlations of δ^2H with grain yield illustrate that this isotope can be used to assess plant performance under different growing conditions.

Analyses of the stable isotope ratios of carbon and oxygen in plant material have been applied in time-integrated approaches for climatological, ecological, or biochemical research in plant science (Dawson et al., 2002; Barbour, 2007; Gessler et al., 2014), including the evaluation of crop performance under different environmental conditions (Richards, 1996; Farquhar et al., 1998, 2007; Barbour and Farquhar, 2000; Araus et al., 2003, 2013; Cabrera-Bosquet et al., 2009a, 2011). The stable isotope ratio of hydrogen in plant material has also been examined in different areas of plant research (Dawson et al., 2002). However, it has not been exploited in crop research to the same degree.

The carbon isotope composition ($\delta^{13}C$) of plant dry matter (DM), frequently expressed as a discrimination from surrounding air ($\Delta^{13}C$), has been used for decades as a tool for screening plants with high water use efficiency during the assimilate deposition period, due to the well-established link between $\Delta^{13}C$ and the intercellular versus the atmospheric partial pressure of CO_2 (Farquhar and Richards, 1984; Farquhar et al., 1989; Richards et al., 2002). In C_3 plants, ^{13}C discrimination mainly occurs during two steps of CO_2 uptake: (1) CO_2 diffusion from the air to the intercellular air space through the boundary layer and stomata, and (2) the carboxylation reaction by Rubisco (Farquhar et al., 1982). In addition, the water regime strongly affects the carbon isotope signature of the plant, with drought increasing $\delta^{13}C$ due to low stomatal conductance-driven CO_2 diffusion (Araus et al., 2003; Condon et al., 2004). However, the effects of other growing factors such as nitrogen (N) availability on $\delta^{13}C$ remain unclear, and contradictory results have been reported. Thus, the $\delta^{13}C$ in wheat (*Triticum* spp.) has been observed either to decrease (Shangguan et al., 2000; Zhao et al., 2007), increase (Zhao et al., 2007;

[1]This work was supported by the Ministry of Economy and Competitiveness (MINECO), Spain (project AGL2016-76527-R) and by the Catalan Institution for Research and Advanced Studies (ICREA) Academia, Government of Catalonia, Spain to J.L.A.

[2]Present address: Department of Crop and Forest Sciences, University of Lleida and AGROTECNIO (Centre for Research in Agrotechnology), Lleida, Spain 25198.

[3]Author for contact: jaraus@ub.edu.

[4]Senior author.

The author responsible for distribution of materials integral to the findings presented in this article in accordance with the policy described in the Instructions for Authors (www.plantphysiol.org) is: José Luis Araus (jaraus@ub.edu).

R.S.B. and J.L.A. conceived and designed the study. R.S.B., J.B., and M.D.S. carried out the field measurements. R.S.B. and R.M.M. conducted laboratory work. R.S.B. and J.L.A. analyzed the data; R.S.B. and J.L.A. interpreted the results. R.S.B. took the principal role in writing the article. All authors have contributed to the revision of the article.

www.plantphysiol.org/cgi/doi/10.1104/pp.19.00238

Serret et al., 2008; Cabrera-Bosquet et al., 2009a), or be unaffected (Hubick et al., 1990) as N supply increases. Furthermore, the interaction of nitrogen fertilization and water regime may affect $\delta^{13}C$ (Araus et al., 2013).

During recent years, interest has grown in using oxygen isotope composition ($\delta^{18}O$) in plant matter because it integrates evaporative conditions during the crop cycle (Barbour et al., 2000; Barbour, 2007). It is known that the $\delta^{18}O$ of leaf water (and organic matter that carries leaf water signal) becomes isotopically enriched during transpiration (Barbour and Farquhar, 2000). Indeed, under common environmental conditions (where the $\delta^{18}O$ of ambient vapor, ambient moisture content, and source water do not vary across different plants), the interest in $\delta^{18}O$ is motivated by the concept that $\delta^{18}O$ may be affected by transpiration, which simultaneously depends on stomatal conductance (g_s; Barbour and Farquhar, 2000; Helliker and Ehleringer, 2002). Similar to $\delta^{18}O$, the effect of environment on transpiration and evaporation also drives leaf water evaporative ^2H-enrichment in the plant (Smith and Freeman, 2006; Feakins and Sessions, 2010; Kahmen et al., 2013; Cernusak et al., 2016). Therefore, the plant δ^2H in organic matter is not only influenced by g_s, but also by the effects of climate on transpiration (Sternberg et al., 1984; Cernusak et al., 2016). Thus, a high correlation between $\delta^{18}O$ and δ^2H in organic matter may indicate the source (i.e. water) and environmental effects (Epstein et al., 1977), whereas a lack of correlation would suggest either an additional hydrogen (Sternberg et al., 1986) or oxygen (Barbour, 2007) isotope fractionation effect.

Theoretically, as driving factors, g_s and leaf temperature can influence several parameters of the $\delta^{18}O$ and δ^2H leaf water enrichment model, either directly or indirectly (Flanagan et al., 1991; Farquhar and Lloyd, 1993). The model relates the enrichment of $\delta^{18}O$ and δ^2H in leaf water above the source of water during evaporation to (1) the kinetic fractionation during diffusion through the stomata such as e_a/e_i (through its influence on leaf temperature; Farquhar et al., 2007), (2) the Péclet number (through its influence on transpiration; Cuntz et al., 2007), (3) the leaf boundary layer, ε_k (the kinetic fractionation that occurs during diffusion and through the pores of the stomata in the leaf layer), and (4) ε^+ (the proportional depression of water vapor pressure by the heavier $H_2{}^{18}O$ molecule), which is dependent on temperature.

As indicated previously, ^{18}O is enriched in leaves or other transpiring organs relative to the source water (Gonfiantini et al., 1965; Farquhar et al., 1989; Pande et al., 1995). Even so, diverse factors can affect the use of $\delta^{18}O$ to assess plant performance (Barbour and Farquhar, 2000; Sánchez-Bragado et al., 2016). Thus, the $\delta^{18}O$ of photoassimilates may be affected by the isotopic composition of the water source available to the plant (Yakir et al., 1990a; Roden et al., 2000; Williams et al., 2005), by the plant height and leaf length (Helliker and Ehleringer, 2000, 2002) or by fractionation during postphotosynthetic processes due to biochemical reactions involved in the synthesis of organic matter (Farquhar and Lloyd, 1993) and its subsequent transport within the plant (Offermann et al., 2011). However, some studies have observed that there is no fractionation during Suc transport (Cernusak et al., 2005), although biochemical fractionation can be impacted by physiological processes such as the carbon turnover rate, which may affect the $\delta^{18}O$ of organic matter (Song et al., 2014). Nonetheless, $\delta^{18}O$ has been used to evaluate plant responses to different water regimes in cereals such as maize (*Zea mays*) and wheat (Barbour et al., 2000; Barbour, 2007; Cabrera-Bosquet et al., 2009b; Araus et al., 2013). However, studies combining the effects of N supply and water regime on $\delta^{18}O$ are still scarce, and the results are contradictory (Cernusak et al., 2007; Cabrera-Bosquet et al., 2009a, 2011; Araus et al., 2013).

Similar to $\delta^{18}O$, δ^2H in plant organic compounds is affected by the water source (Epstein et al., 1977; Sternberg et al., 1984; Chikaraishi and Naraoka, 2003; Sachse et al., 2006; Schwendenmann et al., 2015). However, an important factor that determines the δ^2H but not the $\delta^{18}O$ in plant organic compounds is related to the biochemical processes between organic compounds and cellular water, which may cause biosynthetic fractionation of ^2H (Ziegler et al., 1976; Sternberg et al., 1984; Ziegler, 1989; Yakir and Deniro, 1990; Luo and Sternberg, 1991; Yakir, 1992). Unlike $\delta^{18}O$, the δ^2H of organic matter is also affected by carbon metabolism; and it has been proposed, for example, as a proxy to assess crassulacean acid metabolism (CAM) metabolism in plants (Sternberg et al., 1984). Thus, photosynthesis has a major impact on the δ^2H of plant organic matter (Ziegler et al., 1976; Luo et al., 1991; Yakir, 1992; Schmidt et al., 2003; Sachse et al., 2012). Although the mechanisms related to the effects of photosynthetic metabolism on plant δ^2H are insufficiently understood (Sachse et al., 2012), these mechanisms seem clearly different from those determining $\delta^{13}C$ and $\delta^{18}O$. Thus, the photosynthetic H fractionation processes that occur during NADPH formation in the photosynthetic light reactions and triose phosphate primary assimilation may also contribute to determining the δ^2H in plant organic compounds (Roden et al., 2000). In fact, the NADPH produced during photosynthesis has been observed as being extremely depleted in ^2H (Luo et al., 1991; Schmidt et al., 2003). Moreover, it has been reported that recently produced autotrophic cellulose in leaves might be depleted in ^2H compared with available water (Yakir et al., 1990a; Luo et al., 1991). The reason for such depletion might be related to reduction reactions, whereby the NADPH-derived hydrogen that is added to carbon skeletons seems strongly depleted (on average) relative to water (Sachse et al., 2012). Conversely, during heterotrophic metabolism, all other reactions following the primary assimilation of triose phosphate may enrich the ^2H of plant organic matter (Roden et al., 2000) due to the exchange of a large proportion of hydrogen atoms with surrounding water (Ziegler, 1989). In addition, postphotosynthetic

^{2}H-fractionation processes may also occur via the oxidative pentose phosphate pathway during sugar metabolism. Thus, the NADPH produced may be more enriched (i.e. less depleted) in ^{2}H (Yakir and Deniro, 1990; Schmidt et al., 2003). Hence, photosynthesis depletes the ^{2}H of the carbon-bound hydrogen carbohydrates (the fractionation factor is around −200‰), whereas postphotosynthetic metabolism has the opposite effect (+150‰; Yakir, 1992; Sachse et al., 2012). Nonetheless, until now there has not been a clear understanding of the photosynthetic and postphotosynthetic biochemical processes that determine δ^2H fractionation during plant organic biosynthesis. In fact, there have been fewer applications of hydrogen isotope ratios compared with the other stable light isotopes in studies of plant organic matter. The underlying reason is related to the presence of isotopically exchangeable atoms of hydrogen in the organic compounds (oxygen in the DM can also exchange with moisture, although such an effect is predicted to be much smaller than for δ^2H; Yousfi et al., 2013). The percentage of hydrogen atoms of cellulose that are exchangeable can reach 30% (isotopes of hydrogen bound to oxygen in hydroxyl groups), whereas the remaining 70% are nonexchangeable hydrogen atoms bound to carbon (Filot et al., 2006). Therefore, the hydroxyl hydrogen group can easily exchange with environmental water sources, complicating the interpretation of this isotope in plant organic matter. Nevertheless, developments in isotope-ratio mass spectrometry for compound-specific analyses have promoted the use of H isotopes.

In summary, δ^2H in plants may share some commonalties in terms of factors affecting its signature, with δ^{18}O (affected by transpiration and the signature of the source water) and even with δ^{13}C (through g_s), which are both triggered by environmental factors (for example, the availability of water). However, δ^2H may be further strongly affected by the trophic (photoautotrophic versus heterotrophic) nature of the plant part considered. In the case of a leaf (or another photosynthetic organ), the δ^2H in carbohydrates will be a balance between autotrophic and heterotrophic processes (Yakir et al., 1990b). Therefore, although there is no evidence that the fractionation effect of δ^2H is associated with environmental stress, the effect of any environmental stress on the photosynthetic activity might eventually affect the final δ^2H in the carbohydrates of the plant.

The objective of this study was to evaluate the influence of growing conditions on transpiration and how these circumstances affect the δ^2H of autotrophic (leaves), mixotrophic (ears), and heterotrophic (roots and mature kernels) organs compared with the δ^{13}C and δ^{18}O in DM and the water-soluble fraction (WSF) in the same organs. For this case study, durum wheat (*Triticum turgidum* var *durum*) was chosen due to its frequent exposure to the vagaries of abiotic stress. Durum wheat is among the main crops cultivated in the Mediterranean basin (Food and Agriculture Organization of the United Nations (FAOSTAT), 2017) where production areas are often simultaneously exposed to water stress (Lobell et al., 2008) and low N availability (Oweis et al., 1998; Sadras, 2004). Moreover, there is increasing evidence that ongoing climate change is already stagnating productivity (Moore and Lobell, 2015; Ceglar et al., 2016) by decreasing precipitation while increasing evapotranspiration. Thus, a panel of modern cultivars and landraces of durum wheat were grown in the field during two consecutive years under different combinations of water and nitrogen fertilization. To the best of our knowledge there have been no field studies in crop species reporting on the variation in δ^2H within different organs and among genotypes under a combination of different water and nitrogen conditions; and therefore, comparisons among these three stable light isotopes (^{13}C, ^{2}H, and ^{18}O) as ecophysiological indicators of plant performance are absent.

RESULTS

Average grain yield (*GY*), including all growing conditions, was higher in 2011 (3.1 Mg·ha^{-1}) compared with that in 2010 (1.7 Mg·ha^{-1}; data not shown). Similarly, cultivars showed higher *GY* (1.9 Mg·ha^{-1} and 3.1 Mg·ha^{-1} for 2010 and 2011, respectively) compared with that in landraces (1.5 Mg·ha^{-1} and 1.6 Mg·ha^{-1} for 2010 and 2011, respectively) during both growing seasons. Moreover, the *GY* of both landraces and cultivars was higher under support irrigation (SI) than rainfed (RF) conditions (Tables 1 and 2). Furthermore, whereas g_s was much higher under SI compared with that under RF conditions in 2010 and 2011 (Tables 1 and 2), no significant differences were observed between landraces and cultivars in 2010 (Table 1). In contrast, in 2010, g_s decreased in response to nitrogen fertilization (Table 1).

Hydrogen, Oxygen, and Carbon Isotope Composition across Tissues

Mean values averaged across genotypes of stable hydrogen (δ^2H), oxygen (δ^{18}O), and carbon (δ^{13}C) isotope composition within different tissues (Fig. 1). Hydrogen isotopic composition in mature grains showed the most enriched (less negative) values (δ^2H_{grain} = −32.4‰) compared with that in the ears ($\delta 2H_{ear}$ DM = −92.4‰), flag leaves (δ^2H_{flag}DM = −115.2‰), and roots ($\delta 2H_{roots}$ DM = −67.0‰). For the δ^{13}C, the ears ($\delta^{13}C_{ear}$ DM = −24.7‰) and mature grains ($\delta^{13}C_{grain}$ = −24.3‰) showed the most enriched values compared with that in the flag leaves ($\delta 13C_{flag}$ DM = −25.7‰; Fig. 1). In the case of δ^{18}O, the most enriched tissue was the flag leaf ($\delta 18O_{flag}$ DM = 30.6‰).

Hydrogen isotope composition of stem water ($\delta 2H_{stem\ W}$ = −45.9‰) was depleted compared to that of the grain DM, but enriched compared with that of the flag leaves (WSF), the ears (WSF), and the roots (DM;

Table 1. *Mean values of* GY, g_s, *and stable isotope compositions (‰) of* δ^2H, $\delta^{18}O$, *and* $\delta^{13}C$

Mean values of *GY*, g_s, and stable isotope composition (‰) of δ^2H, $\delta^{18}O$, and $\delta^{13}C$ of DM and the WSF of different plant parts (flag leaves, ears, and roots) sampled at mid-grain-filling plus mature kernels (grains) and in the water from the basal part of the stem [stem water (stem W)] under SI, RF, N fertilized (HN), and nonfertilized (LN) conditions, as examined in modern cultivars (cultivars) and old landraces (landraces) We measured $\delta^{13}C$ DM and $\delta^{13}C$ WSF, and $\delta^{18}O$ WSF and δ^2H WSF in 108 plots (five cultivars and four landraces, four growing conditions and three replicates); whereas we measured $\delta^{18}O$ DM and δ^2H DM in 48 plots (two cultivars and two landraces, four growing conditions and three replicates) during the 2010 crop cycle. Each value represents the mean ±SD. Mean values across plant tissues with different letters (a and b) are significantly different from SI versus RF and HN versus LN, and landraces versus cultivars, according to Tukey's Honest Significant Difference Test ($P < 0.05$).

Isotope/Organ/Fraction	Cultivars	Landraces	SI	RF	HN	LN
Hydrogen						
δ^2H_{roots} DM	−67.1 ± 18.6a	−73.2 ± 20.6a	−64.3 ± 23.5a	−75.8 ± 13.3b	−72.5 ± 17.7a	−68.0 ± 21.5a
$\delta^2H_{stem\ W}$	−46.4 ± 7.2a	−45.3 ± 5.7a	−46.3 ± 7.6a	−45.6 ± 5.6a	−47.1 ± 7.3a	−44.8 ± 5.7a
$\delta2H_{flag}$ DM	−114.9 ± 8.7a	−115.5 ± 8.8a	−120.6 ± 6.7a	−109.6 ± 6.8b	−111.5 ± 9.6a	−119.1 ± 5.5b
$\delta2H_{flag}$ WSF	−100.9 ± 6.9a	−104.4 ± 7.4b	−104.1 ± 7.8a	−100.9 ± 6.4b	−101.8 ± 8.1a	−103.2 ± 6.4a
$\delta2H_{ear}$ DM	−90.0 ± 8.6a	−95.3 ± 10.6a	−99.0 ± 7.1a	−86.4 ± 8.1b	−88.9 ± 10.0a	−96.4 ± 8.4b
$\delta2H_{ear}$ WSF	−65.7 ± 7.0a	−71.4 ± 9.2b	−72.5 ± 6.7a	−64.3 ± 8.0b	−65.4 ± 9.5a	−71.2 ± 6.4b
δ^2H_{grain}	−33.6 ± 8.2a	−30.9 ± 9.4a	−36.6 ± 6.6a	−28.2 ± 8.9b	−27.4 ± 7.7a	−35.8 ± 6.9b
Oxygen						
$\delta18O_{roots}$ DM	28.1 ± 7.5a	30.8 ± 8.8a	29.6 ± 9.0a	29.3 ± 7.6a	32.3 ± 9.4a	26.7 ± 5.9b
$\delta^{18}O_{stem\ W}$	−6.3 ± 1.0a	−6.1 ± 0.6a	−6.4 ± 0.9a	−6.0 ± 0.8a	−6.4 ± 0.9a	−6.0 ± 0.7a
$\delta18O_{flag}$ DM	0.8 ± 1.7a	31.0 ± 1.1a	30.3 ± 1.0a	31.4 ± 1.6b	31.1 ± 1.6a	30.7 ± 1.3a
$\delta18O_{flag}$ WSF	30.7 ± 2.2a	30.0 ± 2.3a	28.9 ± 1.9a	32.3 ± 0.9b	29.6 ± 2.7a	31.2 ± 1.3a
$\delta^{18}O_{ear}$ DM	26.6 ± 2.4a	26.1 ± 2.6a	26.5 ± 2.0a	26.2 ± 2.9a	26.7 ± 2.2a	26.0 ± 2.7a
$\delta^{18}O_{ear}$ WSF	30.9 ± 1.1a	29.9 ± 1.0a	30.2 ± 0.9a	30.7 ± 1.3a	30.3 ± 1.2a	30.7 ± 1.1a
$\delta^{18}O_{grain}$	30.4 ± 0.7a	30.6 ± 0.9b	30.4 ± 0.7a	30.6 ± 0.9a	30.3 ± 0.6a	30.7 ± 0.9a
Carbon						
$\delta^{13}C_{flag}$ DM	−25.9 ± 0.9a	−25.5 ± 0.9b	−26.2 ± 0.7a	−25.2 ± 0.8b	−25.3 ± 0.8a	−26.2 ± 0.8b
$\delta^{13}C_{flag}$ WSF	−27.0 ± 1.1a	−27.2 ± 1.1a	−27.9 ± 0.9a	−26.3 ± 0.7b	−27.2 ± 1.4a	−26.9 ± 0.7a
$\delta13C_{ear}$ DM	−24.5 ± 1.0a	−25.0 ± 0.9b	−25.4 ± 0.7a	−24.1 ± 0.8b	−24.5 ± 1.0a	−25.0 ± 0.9b
$\delta^{13}C_{ear}$ WSF	−23.3 ± 0.9a	−24.4 ± 1.0b	−24.5 ± 0.9a	−23.1 ± 0.8b	−23.6 ± 1.1a	−24.0 ± 1.1a
$\delta^{13}C_{grain}$	−24.6 ± 0.9a	−23.9 ± 1.0b	−25.0 ± 0.6a	−23.5 ± 0.7b	−24.0 ± 1.1a	−24.6 ± 0.8b
g_s (mmol·H_2O·$m^{-2}s^{-1}$)	184.7 ± 78.1a	170.2 ± 59.0a	222.8 ± 56.2a	133.8 ± 52.8b	163.6 ± 84.5a	193.1 ± 49.0b
GY (Mg·ha^{-1})	1.9 ± 0.1a	1.5 ± 0.1b	2.1 ± 0.1a	1.3 ± 0.1b	1.8 ± 0.1 a	1.6 ± 0.1 a

Fig. 2). In contrast, the $\delta^{18}O$ of stem water ($\delta18O_{stem\ W}$ = −5.6‰) displayed the most depleted value regardless of the tissues and fractions (DM, WSF) analyzed (Fig. 2). Moreover, the δ^2H and $\delta^{18}O$ of stem water were more depleted compared with that of grain water ($\delta2H_{grain\ W}$ = −15.3‰ and $\delta18O_{grain\ W}$ = 7.0‰) and flag leaf water ($\delta^2H_{flag\ W}$ = 9.2‰ and $\delta^{18}O_{flag\ W}$ = 11.3‰; Fig. 2).

Fractionation of Hydrogen, Oxygen, and Carbon Isotope Composition across Plant Tissues

In order to further assess whether similar fractionation processes affected isotopic composition of hydrogen, oxygen, and carbon within the plant, a correlation analysis was performed between different isotope compositions ($\delta^{18}O$, $\delta^{13}C$, and δ^2H) in the WSF of the same plant tissue (mature kernels, ears, and flag leaves; Fig. 3). The strongest relationship in the flag leaf WSF (left columns of Fig. 3) was observed between $\delta^{18}O$ and $\delta^{13}C$ (r = 0.87, $P < 0.001$); whereas in the WSF of the ears, the strongest correlation was found between δ^2H and $\delta^{13}C$ (r = 0.74, $P < 0.001$), followed by $\delta^{18}O$ and $\delta^{13}C$ (r = 0.65, $P < 0.001$). In mature kernels, δ^2H and $\delta^{13}C$ were highly correlated (r = 0.70, $P < 0.001$), whereas $\delta^{18}O$ did not correlate with either δ^2H or $\delta^{13}C$.

In order to estimate whether the fractionation processes affecting δ^2H and $\delta^{18}O$ were similar in the water transported by different plant tissues, a correlation analysis was performed between the oxygen and hydrogen isotope compositions of the water extracted from different tissues (Table 3). The result showed that $\delta^2H_{flag\ W}$ was positively correlated with $\delta^2H_{grain\ W}$ (r = 0.66, $P < 0.001$), whereas no correlation was observed with $\delta^2H_{stem\ W}$. Similarly, $\delta^{18}O_{flag\ W}$ was positively correlated with $\delta^{18}O_{grain\ W}$ (r = 0.67, $P < 0.001$) but not with $\delta^{18}O_{stem\ W}$. In addition, in order to estimate whether the same fractionation processes affected δ^2H and $\delta^{18}O$ in the water of tissues, correlation analyses between the δ^2H and $\delta^{18}O$ of the water in the same tissues were performed (Table 3). It was observed that the δ^2H and $\delta^{18}O$ in flag leaf water were strongly correlated (r = 0.99, $P < 0.001$). Similarly, δ^2H and $\delta^{18}O$ were strongly correlated in the grain water (r = 0.99, $P < 0.001$) and stem water (r = 0.81, $P < 0.001$).

Water and Nitrogen Effects on Carbon, Oxygen, and Hydrogen Isotope Composition

Significant differences within SI and RF conditions (Table 1) were mainly observed in δ^2H and $\delta^{13}C$ in 2010. Concerning $\delta^{18}O$, only the flag leaf DM or the flag leaf

Table 2. *Mean values of* GY, g_s, *and carbon, oxygen, and hydrogen stable isotope compositions*

Hydrogen isotope composition (‰) was analyzed in the flag leaf water ($\delta^2H_{flag\ W}$), grain water ($\delta^2H_{grain\ W}$), stem water ($\delta^2H_{stem\ W}$), and irrigation water ($\delta^2H_{source\ W}$) in SI plots. Oxygen isotope composition (‰) was analyzed in the flag leaf water ($\delta^{18}O_{flag\ W}$), grain water ($\delta^{18}O_{grain\ W}$), stem water ($\delta^{18}O_{stem\ W}$), irrigation water in SI ($\delta^{18}O_{source\ W}$), and the DM of the flag leaves ($\delta^{18}O_{flag}$ DM) and mature kernels ($\delta^{13}C_{grain}$). Carbon isotope composition (‰) was analyzed in the DM in the flag leaves ($\delta^{13}C_{flag}$ DM) and mature kernels ($\delta^{13}C_{grain}$). We performed δ^{13}C analysis on nine durum wheat genotypes and three replicates grown under two different water conditions (SI versus RF, including all levels of N), accounting for a total of 54 plots. For water extracted from flag leaves, δ^{18}O and δ^2H were measured in a subset of two cultivars and two landraces (with three replicates) under fertilized conditions and two water regimes (18 plots). We measured δ^{18}O and δ^2H in extracted water from stems, developing grains and DM in a subset of five cultivars and five landraces (with three replicates) under fertilized conditions and two water regimes (45 plots) during the 2011 crop cycle (landraces were discarded due to lodging under SI conditions; see the "Materials and Methods" section). Each value represents the mean ±SD. Mean values across plant tissues with different letters (a and b) are significantly different according to Tukey's Honest Significant Difference Test ($P < 0.05$). Dashes indicate no data.

Isotope/Water Organ	*SI*	*RF*
Hydrogen		
$\delta^2H_{flag\ W}$	−8.1 ± 0.4a	17.9 ± 2.4b
$\delta^2H_{grain\ W}$	−26.2 ± 0.9a	−9.7 ± 2.3b
$\delta^2H_{stem\ W}$	−43.0 ± 0.6a	−43.8 ± 0.6a
$\delta^2H_{source\ W}$	−45.0	–
Oxygen		
$\delta^{18}O_{flag\ W}$	3.0 ± 0.5a	15.5 ± 1.0b
$\delta^{18}O_{grain\ W}$	2.8 ± 0.2a	9.3 ± 0.7b
$\delta^{18}O_{stem\ W}$	−5.6 ± 0.1a	−5.6 ± 0.1a
$\delta^{18}O_{source\ W}$	−6.1	–
$\delta^{18}O_{flag}$ DM	27.7 ± 0.1a	33.3 ± 0.2b
$\delta^{18}O_{grain}$	30.2 ± 0.1a	32.3 ± 0.1b
Carbon		
$\delta^{13}C_{flag}$ DM	−28.8 ± 0.1a	−26.5 ± 0.1b
$\delta^{13}C_{grain}$	−26.3 ± 0.1a	−24.4 ± 0.1b
g_s (mmol·H_2O·$m^{-2}s^{-1}$)	110.0 ± 36.3	29.1 ± 22.5
GY (Mg·ha^{-1})	4.5 ± 0.1a	1.7 ± 0.1b

WSF showed significant differences between the two water regimes in 2010. Overall, water stress tended to increase δ^2H, δ^{18}O, and δ^{13}C irrespective of the tissue or fraction analyzed, with the exception of $\delta 2H_{roots}$ DM (Table 1). Furthermore, fertilized plants (HN) showed higher δ^2H and δ^{13}C compared with that in to nonfertilized plants (LN), although no significant differences were observed in $\delta 2H_{roots}$ DM, $\delta^2H_{stem\ W}$, and $\delta 13C_{flag}$WSF. By contrast, δ^{18}O did not exhibit significant differences among fertilization conditions, with the exception of in the roots (δ^2H_{roots} DM).

Carbon, Oxygen, and Hydrogen Isotope Composition in Cultivars and Landraces

Overall, the δ^2H in 2010 was lower in landraces compared with cultivars (Table 1), although significant differences were only observed in the δ^2H of the WSF of the flag leaf and ear. A similar trend was exhibited by δ^{13}C, with landraces having lower δ^{13}C compared with cultivars, with the exception of $\delta^{13}C_{flag}$ DM (Table 1). Conversely, $\delta^{13}C_{grain}$ and δ^2H_{grain} were less enriched in landraces compared with cultivars. There were no significant differences in δ^{18}O, regardless of the organs and fractions considered, with the exception of in the grains (Table 1).

Correlations of δ^2H, δ^{18}O, and δ^{13}C with *GY*, g_s, and N Content

The δ^2H, δ^{18}O, and δ^{13}C in DM and WSF from different tissues plus mature kernels were correlated with *GY*, g_s, and N content in the flag leaves (N-Flag) and the ears (N-Ear). Correlations were calculated including all genotypes and either (1) across the whole set of growing conditions in 2010 (Fig. 4), or (2) across different water regimes for a given nitrogen fertilization level (HN and LN), or (3) across nitrogen regimes within each water condition (SI and RF; Table 4). In general, δ^2H and δ^{13}C in the different tissues and water were negatively correlated with *GY* ($P < 0.05$) and g_s ($P < 0.01$) when all genotypes and growing conditions were combined (Fig. 4) and across the four different combinations of water and nitrogen regimes (SI, RF, HN, and LN; Table 4), with δ^{13}C in mature grains showing the highest correlation against *GY* when all growing conditions were included (Fig. 4). Conversely, δ^2H and δ^{13}C were positively correlated with N-Flag ($P < 0.01$) and N-Ear ($P < 0.01$) under SI and RF conditions (Table 4); whereas under HN conditions, this correlation was negative (Table 4). With regard to δ^{18}O, it was marginally correlated with *GY*, g_s, N-Flag, and N-Ear in 2010 (Fig. 4; Table 4). However, when all growing conditions were combined in 2011 (Table 3), *GY* was negatively and strongly correlated with $\delta^{18}O_{flag}$ DM ($P < 0.001$) as well as with $\delta^{18}O_{flag\ W}$ ($P < 0.001$). Additionally, correlations of $\delta^{18}O_{grain\ W}$ with *GY* were also observed ($P < 0.001$; Table 3).

Furthermore, in order to test which isotope, tissue, and fraction better explained yield, a stepwise regression analysis was performed in the 2010 trials between the analyzed signatures of the different isotopes, tissues, and fractions (either DM and WSF) as independent variables and with *GY* as the dependent variable (Table 5). The stepwise analysis was performed combining all treatments together (global) for each of the water regimes and both fertilization levels together (SI, RF) and for each N fertilization level and both water regimes combined (HN, LN). In the global and HN analyses, the first independent variable chosen by the model was $\delta^{13}C_{grain}$, whereas in the LN analysis, it was the $\delta^{18}O_{flag}$ WSF. Conversely, in the SI and RF analyses, δ^2H_{ear} WSF and δ^2H_{grain} were the first variables chosen by the model, respectively.

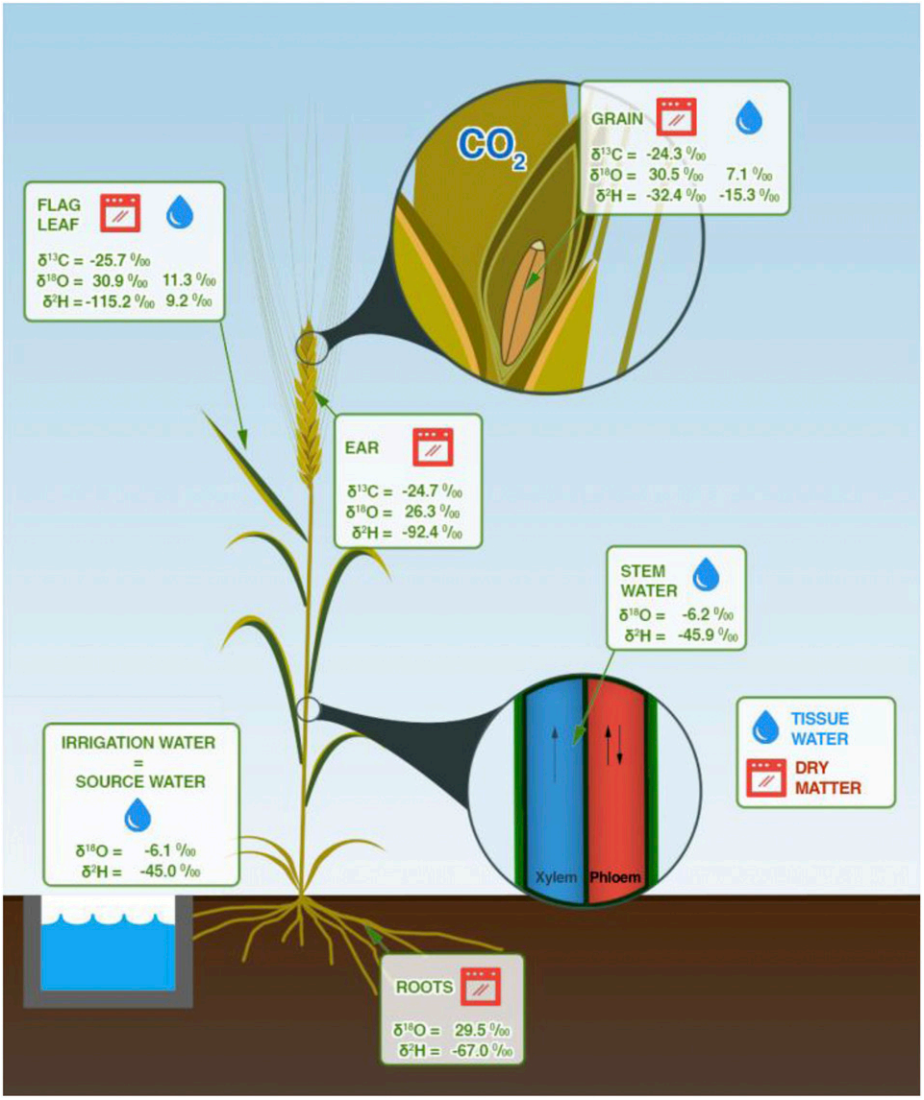

Figure 1. Illustration of a wheat plant and the stable isotope composition (‰) of δ^2H, $\delta^{18}O$, and $\delta^{13}C$ of different plant parts (flag leaves, ears, and roots) sampled at mid-grain-filling, plus mature kernels (grains) and the water (blue drops) from the basal part of the stems, flag leaves, and developing grains. Values presented are means from the DM of five representative plants per plot and including all treatments. We measured $\delta^{13}C$ DM in 108 plots (five cultivars and four landraces, four growing conditions, and three replicates); whereas we measured $\delta^{18}O$ DM and δ^2H DM in 48 plots (two cultivars and two landraces, four growing conditions, and three replicates) during the 2010 crop cycle. The $\delta^{18}O$ and δ^2H of the water extracted from the flag leaves were analyzed in a subset of two cultivars and two landraces (with three replicates) under fertilized conditions and two water regimes (18 plots; landraces in SI conditions were discarded due to lodging). We measured $\delta^{18}O$ and δ^2H in water from the stems, developing grains and DM in a subset of five cultivars and five landraces (with three replicates) under fertilized conditions and two water regimes (45 plots; landraces were discarded due to lodging under SI conditions; see "Materials and Methods" section). Analyses of water extracted from different tissues were performed in samples from the 2011 crop season.

Experimental Estimation of the Electron Transport Rate's Association with δ^2H Depletion

The δ^2H and $\delta^{13}C$, together with g_s and the electron transport rate (ETR), were assessed in the flag leaves of the same durum wheat variety growing under controlled conditions under two different relative humidity (RH) conditions (40% and 80% RH). Plants growing under 80% RH showed depleted $\delta^{13}C$ values and higher g_s in the flag leaves compared to that in plants grown under 40% RH. Accordingly, flag leaves exhibited more depleted δ^2H values and higher ETR under 80% RH, compared with that under 40% RH (Supplemental Table S1).

DISCUSSION

Photosynthetic Fractionation and Autotrophic Effects

Similar to the effect on $\delta^{13}C$, photosynthesis could have a major impact on δ^2H (Sternberg et al., 1984). In our study, the δ^2H from the flag leaf water showed enriched values compared with that of δ^2H_{flag} (either DM or WSF), indicating that depleted values of the δ^2H_{flag} in plant matter or the WSF may not originate from evaporative processes, but are mainly due to photosynthetic reactions. In fact, δ^2H_{flag} WSF versus $\delta^{13}C_{flag}$ WSF were better correlated than δ^2H_{flag} WSF versus $\delta^{18}O_{flag}$ WSF (Fig. 3), suggesting that leaf δ^2H is not only affected by changes in transpiration and g_s, alongside the evaporative conditions (Cernusak et al., 2016), but also by photosynthetic reactions (Yakir et al., 1990b) and carbon metabolism in plants (Cormier et al., 2018). Recent autotrophically produced cellulose, lipids (Sternberg, 1988), or starch (Hayes, 2001) in leaves might be depleted in ^2H compared with the available water (Yakir et al., 1990a; Fig. 2). Although the hydrogen isotope composition in the leaf plant water may be imprinted in sugars and metabolites and thus also retained in organic compounds (Cernusak et al., 2016), the isotopic composition of the H transferred

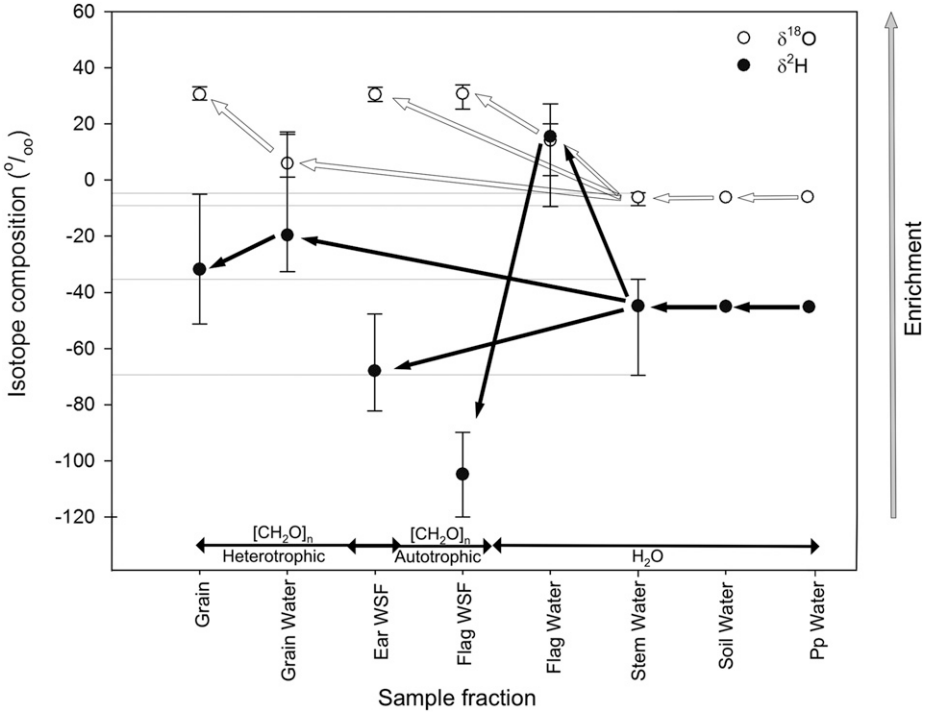

Figure 2. Schematic representation of the major steps in the development of the ratios of oxygen ($\delta^{18}O$) and hydrogen (δ^2H) isotope composition (‰) in plant carbohydrates and tissue water. Data was obtained from the WSF of the flag leaves and ears (flag WSF, ears WSF) and water extracted from different plant tissues (grain water, flag leaf water, and stem water) at mid-grain-filling, plus mature kernels (grains) in nine durum wheat genotypes and three replicates during the 2010 crop cycle. Each value represents the mean ± SD. Arrows represent the change in δ^2H and $\delta^{18}O$ from water sources (including irrigation water, soil water, precipitation water [Pp]) to carbohydrates in autotrophic or heterotrophic tissues. White circles and arrows represent $\delta^{18}O$, black circles and arrows represent δ^2H.

from NADPH to biosynthetic substrates might be one of the most important factors controlling the hydrogen-isotopic composition of organic matter in photosynthetic organs (Hayes, 2001). This evidence was supported and quantified by a study performed by Yakir and Deniro (1990) in *Lemma gibba* grown under autotrophic conditions. In this study, the negative fractionation factor between the water and photosynthates caused a strong depletion (−171‰). Such a low delta value was postulated to be the consequence of the extremely deuterium-depleted protons (Luo et al., 1991; Hoganson and Babcock, 1997) used (from a water molecule within the cell) for the reduction of $NADP^+$ to NADPH. However, in a study performed by Cormier et al. (2018) in different vascular plant species, the increase in light intensity (above 115 μM $m^{-2}s^{-1}$) and consequently the photosynthetic rate, did not clearly deplete the δ^2H in the studied organic compounds. In spite of that, H pools that are strongly depleted relative to leaf water have been observed to result from photosynthetic ^2H fractionation in the chloroplast during light reactions where ferredoxin-$NADP^+$ reductase produces NADPH with reduced H (Luo et al., 1991). The results observed in the growth chamber experiment, with plants grown under two different RH conditions (40% and 80% RH), agree with the findings of Luo et al. (1991); (Supplemental Table S1). Plants growing under 80% RH showed depleted $\delta^{13}C$ values and higher g_s in the flag leaf, suggesting that these plants were exposed to less water-limiting conditions compared with plants grown under 40% RH. Accordingly, flag leaves exhibited more depleted δ^2H values and higher ETRs under 80% RH compared with that under 40% RH (Supplemental Table S1). Because the ETR is associated with a reduction of $NADP^+$ to NADPH during the light reaction of photosynthesis (Foyer et al., 2012) under less water-limiting conditions (80% RH), it is worth considering that there is a causal association of the ETR with the contribution of δ^2H-depleted NADPH to organic δ^2H. In contrast, under more water-limiting conditions (40% RH), the ETR was lower, causing a reduction in NADPH levels and consequently a decrease in the contribution of δ^2H-depleted NADPH to organic δ^2H, resulting in enriched plant organic δ^2H compared with 80% RH. Indeed, the depleted values of δ^2H observed in our experiment in the flag leaves and ears compared with that in the grains would agree with the autotrophic activity of the former organs (Yakir and Deniro, 1990).

Evaporative Fractionation: Transpirative Effects

The δ^2H and $\delta^{18}O$ of water from the flag leaves, ears, and grains were enriched compared with the source of water (water collected from the base of the stem). Indeed, the isotope signature of the water from different plant tissues might influence the isotope signature in the DM and WSF. In our study, the increase in the δ^2H and the $\delta^{18}O$ of the DM and WSF from the flag leaves to the apical part of the plant (flag leaves compared with the ears and grains) may be due in part to the effect of a progressive enrichment in δ^2H and $\delta^{18}O$ of the plant water associated with evaporative demand (Helliker and Ehleringer, 2002). Likewise, $\delta^{18}O_{flag}$WSF and $\delta^{13}C_{flag}$WSF (and $\delta^{18}O_{ear}$WSF and $\delta^{13}C_{ear}$WSF) were strongly correlated, suggesting that in autotrophic organs (leaves and to some extent ears), both isotopes are probably governed by changes in transpiration and g_s,

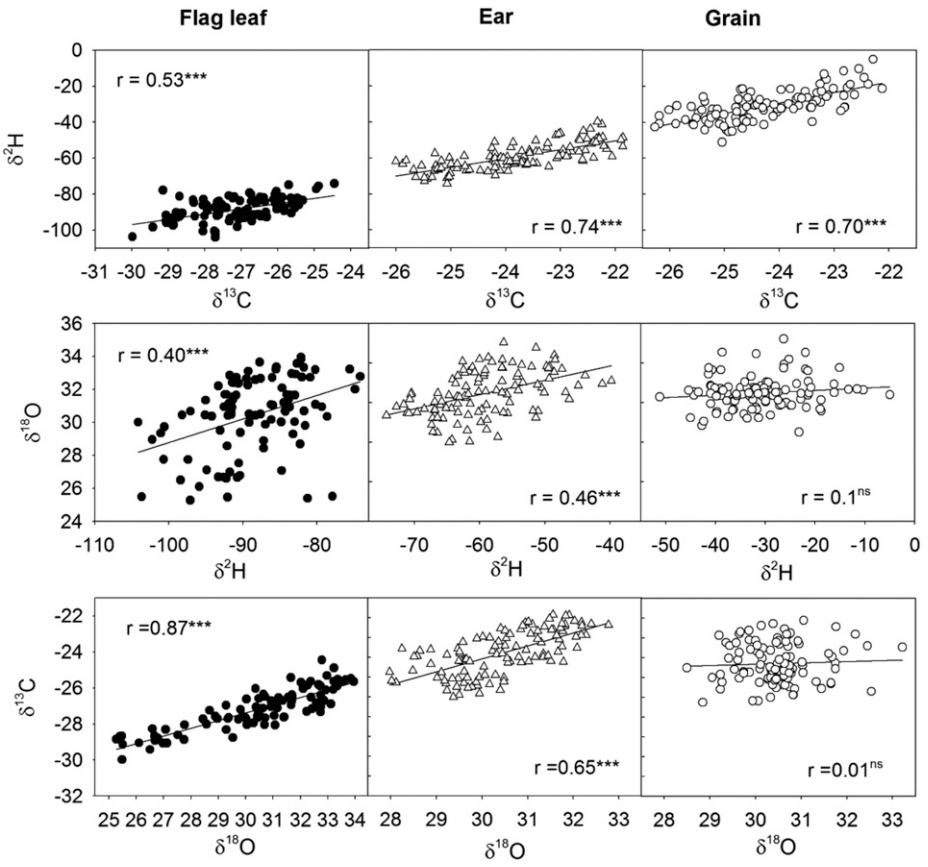

Figure 3. Linear regression of the relationship among the carbon ($\delta^{13}C$), oxygen ($\delta^{18}O$), and hydrogen ($\delta^{2}H$) isotope compositions of the WSF within the flag leaves (left column, closed circles), ears (middle column, white triangles), and mature kernels (right column, white circles). Nine genotypes and three replicates per genotype were considered, accounting for a total of 108 plot values under all growing conditions of the 2010 crop season. Level of significance: ns, not significant, $P > 0.05$; ***, $P < 0.001$.

as previously reported in durum wheat by Cabrera-Bosquet et al. (2009a).

However, in spite of the previously discussed evaporation-driven effect from the bottom to the top of the aerial parts of the plant, the grain water was less enriched in $\delta^{2}H$ and $\delta^{18}O$ compared with that in leaf water, although the grain water was enriched compared with that in the source water. In fact, leaf water (and organic matter that carries the leaf water signal) becomes more ^{2}H enriched than the grains as a result of the evaporative process during transpiration (Craig and Gordon, 1965; Gonfiantini et al., 1965). In the case of water in the grains, different mechanisms may apply. Even if the grains have the photosynthetic "green layer" of aleurone (Caley et al., 1990), few stomata are present on the pericarp (Barlow et al., 1980). In addition, grains are surrounded by the ear bracts, which may therefore minimize transpirative losses (Bort et al., 1996). Moreover, transpiration of the culm, including leaf sheaths, is smaller than in the leaf blades, which may also cause less isotopic enrichment of the water if it goes straight from the base of the stem to the growing grains—rather than, for example, from the base of the stem to the leaf blades (Araus and Tapia, 1987). In addition, there is a xylem discontinuity in the floral axis (Cochrane and Duffus, 1979) and therefore in the longer-term water transport from the stem base to the growing grains. Taking into consideration that transpirative water losses in the grain are low, the acropetal transport of leaf water in the phloem to the developing grains may contribute to enrichment of the $\delta^{2}H$ and $\delta^{18}O$ in the grains relative to the base of the stem as a result of mixing of the phloem water from the leaves with the source water from the base of the stem (Cernusak et al., 2016). In addition, the biphasic enrichment in the grains linked to developmental metabolism of the grain and rapid loss of water during the last part of the grain filling might have enriched the ^{2}H in the grain water compared with that in the source of water (Pande et al., 1994). Indeed, invoking variation in the $\delta^{2}H$ of water among tissues as an explanation for among-tissue (leaf versus grain) variation in DM and the WSF does not seem a convincing conclusion. Further, the "progressive enrichment" concept (Helliker and Ehleringer, 2002) does not appear to hold at the whole-plant level (or at least when comparing leaves with grains).

Moreover, evaporative ^{2}H enrichment of leaf water was markedly higher compared with ^{18}O enrichment. The contrast between the ^{2}H and ^{18}O may be related to the relative magnitude of the equilibrium and kinetic fractionation in the Craig and Gordon model of evaporative site enrichment (Cernusak et al., 2016). The ^{18}O in the leaf water is mainly triggered by kinetic fractionation, whereas equilibrium fractionation mainly dominates ^{2}H (Cernusak et al., 2016). Kinetic effects are closely dependent on stomata and boundary layer resistance (Farquhar et al., 1989), whereas the equilibrium effect varies as a function of temperature (Bottinga and

Table 3. *Linear regressions of the relationships between hydrogen (δ^2H) and oxygen ($\delta^{18}O$) isotope compositions of water from different organs and* GY .

This table shows the linear regression of the relationship between hydrogen isotope composition of the flag leaf water ($\delta^2H_{flag\ W}$), grain water ($\delta^2H_{grain\ W}$) and stem water ($\delta^2H_{stem\ W}$) oxygen isotope composition of the flag leaf water ($\delta^{18}O_{flag\ W}$), grain water ($\delta^{18}O_{grain\ W}$), stem water ($\delta^{18}O_{stem\ W}$), and the DM of the flag leaves ($\delta^{18}O_{flag}$ DM), mature kernels ($\delta^{18}O_{grain}$) and *GY*. Carbon isotope composition is shown for the DM in the flag leaves ($\delta^{13}C_{flag}$ DM), mature kernels ($\delta^{13}C_{grain}$), and *GY*. The $\delta^{18}O$ and δ^2H of the water extracted from the flag leaves were analyzed in a subset of two cultivars and two landraces (with three replicates) under fertilized conditions and two water regimes (18 plots; landraces in SI conditions were discarded due to lodging). The $\delta^{18}O$ and δ^2H were measured in water from the stems, developing grains, and DM in a subset of five cultivars and five landraces (with three replicates) under fertilized conditions and two water regimes (45 plots; landraces were discarded due to lodging under SI conditions; see the "Materials and Methods" section). Analyses were performed in samples from the 2011 crop season. Level of significance: ns, not significant; ***, $P < 0.001$; **, $P < 0.01$; *, $P < 0.05$. Dashes indicate no data.

Isotope/Organ/ Fraction	$\delta^2H_{flag\ W}$	$\delta^2H_{grain\ W}$	$\delta^2H_{stem\ W}$	$\delta^{18}O_{flag\ W}$	$\delta^{18}O_{grain\ W}$	$\delta^{18}O_{stem\ W}$	*GY*
Hydrogen							
$\delta^2H_{flag\ W}$	–	0.66**	−0.13ns	0.99***	0.70**	0.01ns	−0.78***
$\delta^2H_{grain\ W}$	0.65**	–	−0.26ns	0.61**	0.99***	−0.21ns	−0.54***
δ^2H_{stemW}	−0.13ns	−0.26ns	–	−0.12ns	−0.26ns	0.81***	0.12ns
Oxygen							
$\delta^{18}O_{flag\ W}$	0.99***	0.61**	−0.12ns	–	0.67**	0.04ns	−0.82***
$\delta^{18}O_{grain\ W}$	0.70**	0.99***	0.27ns	0.67**	–	−0.20ns	−0.62***
$\delta^{18}O_{stem\ W}$	−0.00ns	−0.21ns	−0.81***	0.04ns	−0.20ns	–	−0.07ns
$\delta^{18}O_{flag}$ DM	0.96***	0.72***	−0.31ns	0.97***	0.82***	0.11ns	−0.93***
$\delta^{18}O_{grain}$	0.90***	0.73***	−0.43*	0.90***	0.80***	0.07ns	−0.83***
Carbon							
$\delta^{13}C_{flag}$ DM	0.89***	0.69***	−0.28ns	0.92***	0.78***	0.16ns	−0.86***
$\delta^{13}C_{grain}$	0.65**	0.49**	−0.08ns	0.71**	0.59***	0.17ns	−0.93***

Craig, 1968). In a study performed in Australia by Kahmen et al. (2013) over a large-scale environmental gradient, the effect of disequilibrium between the source water and atmospheric vapor was stronger for ^2H than that for ^{18}O. (Correlations between the leaf water isotope signature and air RH were stronger for $\delta^{18}O$ than that for δ^2H.) Moreover, under nonequilibrium conditions, evaporative processes tend to cause greater (relative) enrichment of ^{18}O than ^2H; and as a consequence, the slope between δ^2H and $\delta^{18}O$ of water gets flatter (Dansgaard, 1964). However, plants were exposed under steady-state conditions because leaves exhibit relatively open stomata during the day (considering that leaves were not succulent; Cernusak et al., 2008) and therefore these could be assumed as equilibrium conditions. Under such conditions, isotopic enrichment is likely to be stronger for ^2H in the leaf water compared with ^{18}O, causing proportionally higher values in ^2H than ^{18}O in the leaf water.

Postphotosynthetic Fractionation and Heterotrophic Effects

During heterotrophic metabolism, a substantial fractionation of hydrogen isotopes from leaf water to organic matter has been described in Sternberg et al. (1986), a situation that may lead to ^2H enrichment in organic matter (Ziegler, 1989). Postphotosynthetic ^2H enrichment starts in the rapid reciprocal exchange between the triose phosphate pool and the hexosephosphate pool during carbohydrates synthesis (Buchanan et al., 2015; Cormier et al., 2018). Subsequently, there are four processes that lead to ^2H-enrichment of carbohydrates: (1) the synthesis of glyceraldehyde-3-phosphate in the Calvin cycle, which enables exchange with cellular (^2H-enriched) water (Rieder and Rose, 1959); (2) the C-bound H in newly photosynthesized glyceraldehyde-3-phosphate derives from an ^2H-enriched precursor molecule, 3-phosphoglyceraldehyde (due to previous exchange with cellular water); (3) the formation of Fru 1,6-biphosphate from two triose phosphates during hexosephosphate production leads to loss of one of the four C-bound H atoms to the nearby water (Rieder and Rose, 1959), and this action results in an ^2H-enrichment in the glyceraldehyde-3-phosphate pool due to the more rapid reaction of the lighter isotopologues during this process (Schmidt et al., 2015); and (4) the interconversion of Glc 6-phosphate and Fru 6-phosphate, which is performed by the enzyme phosphoglucose isomerase, may also ^2H-enrich glyceraldehyde-3-phosphate pools (Schleucher et al., 1999).

According to our results, the δ^2H of mature grains was enriched compared with that in other analyzed plant parts (including the ear; Fig. 2), and it was also enriched in roots compared with that in flag leaves (Table 1). Only 15% of C-bound H atoms present in carbohydrates in heterotrophic tissues originate from the ^2H-depleted NADPH that is produced during the light reactions of photosynthesis in the chloroplast

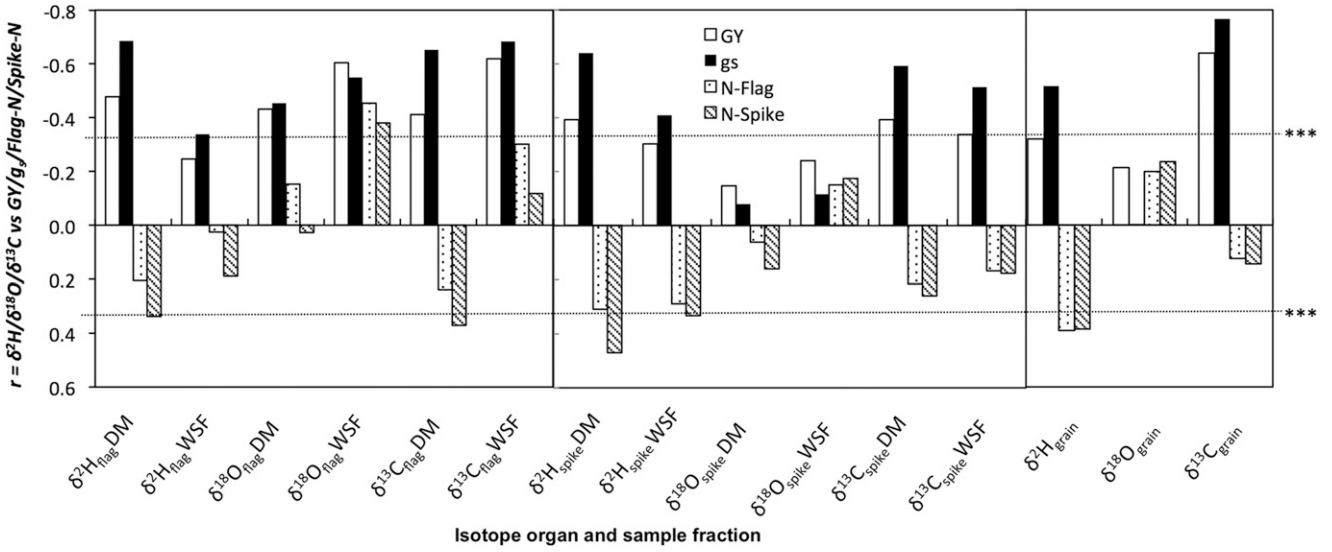

Figure 4. Linear regression of the relationship among the carbon ($\delta^{13}C$), oxygen ($\delta^{18}O$), and hydrogen ($\delta^{2}H$) isotope compositions in mature kernels (grains) and in the DM and WSF of the flag leaves and the ears with the grain yield (*GY*), the stomatal conductance (g_s), and the total N concentration of the flag leaves (N-Flag) and ears (N-Ear). We measured the $\delta^{13}C$ DM and $\delta^{13}C$ WSF, $\delta^{18}O$ WSF and $\delta^{2}H$ WSF in 108 plots (five cultivars and four landraces, four growing conditions and three replicates per genotype and condition), whereas we measured $\delta^{18}O$ DM and $\delta^{2}H$ DM in 48 plots (two cultivars and two landraces, four growing conditions and three replicates) during the 2010 crop cycle. Analyses were performed in samples from the 2010 crop season. Level of significance: ***, $P < 0.001$.

(Cormier et al., 2018), and this result leads to ^{2}H-enriched values in heterotrophic organs such as grains, and specific compounds such as starch or cellulose (Epstein et al., 1976; Sternberg et al., 1984). These findings suggest that $\delta^{2}H$ was exposed to post-photosynthetic enrichment (as explained above) in most heterotrophic organs (such as the grains and roots) in comparison with the more depleted $\delta^{2}H$ in autotrophic organs such as the leaves (Yakir et al., 1990b).

If we follow the same reasoning used for the leaves but with respect to the ear, the $\delta^{2}H$ in the WSF of the ears was depleted compared with mature grains, but enriched compared with the flag leaves (Fig. 2). On one hand, such increases from the flag leaves to the ears could be a consequence of lower g_s in the latter organ (Araus et al., 1993; Tambussi et al., 2005) as well as the result of the mixotrophic nature of the ear bracts (combining large portions of heterotrophic areas with photosynthetic tissues) compared with the leaves (Blum, 1985; Knoppik et al., 1986; Araus et al., 1993; Bort et al., 1994; Li et al., 2006). Furthermore, enriched $\delta^{2}H$ values of the ears in the WSF compared with that in the flag leaves could be a consequence of a degree of CAM metabolism in the ears (Sternberg and Deniro, 1983; Sternberg et al., 1984; Winter et al., 2008; Feakins and Sessions, 2010; Sachse et al., 2012; Winter and Holtum, 2014). Recent studies in wheat glumes and lemmas have shown that the activity of the RuBP carboxylase enzyme decreases significantly in response to water stress, whereas the activity of phosphoenolpyruvate carboxylase increases along with that of NADP-malate dehydrogenase (Jia et al., 2015).

On the other hand, such a decrease in the $\delta^{2}H$ in the DM of the ears with respect to the grains (besides the fact that the grains are subjected to heterotrophic metabolism) could be due to the presence of epicuticular waxes in the ears alongside the support tissues (Araus et al., 1993). In fact, it has been reported in a deciduous conifer that lipids derived from epicuticular waxes and support tissues (e.g. collenchyma and sclerenchyma) are highly depleted in deuterium (Sessions et al., 1999; Chikaraishi et al., 2004; Hou et al., 2007; Yang and Leng, 2009; Zhou et al., 2011) because ^{2}H-depleted NADPH is a critical source of H in lipid biosynthesis (Cormier et al., 2018). Consequently, the presence of lipids derived from cuticular waxes in the DM of the ears might have depleted the $\delta^{2}H$ compared with that in the grains.

Water and Nitrogen Effects on $\delta^{13}C$, $\delta^{18}O$, and $\delta^{2}H$

GY recorded during 2010 and 2011 was in the range reported in earlier work in the Mediterranean basin under dry RF and low supplementary irrigation conditions (Araus et al., 1998, 2003, 2013). SI significantly increased yield, whereas no effect was observed on yield under N fertilization conditions (Table 1).

In our study, N fertilization increased $\delta^{13}C$ and $\delta^{2}H$ in the leaf DM, whereas $\delta^{18}O$ showed a similar trend, although no significant differences were observed. Likewise, an increase in $\delta^{13}C$ due to N fertilization has been reported (Farquhar, 1989) as a consequence of a

Table 4. *Linear regression of the relationship of the $\delta^{13}C$, $\delta^{18}O$, δ^2H isotope compositions and* GY, g_s, *and total N concentration*

Linear regression of the relationship of the $\delta^{13}C$, $\delta^{18}O$, and δ^2H isotope compositions in the WSF and DM of the flag leaves, ears, and mature kernels (grains) with the *GY*, g_s, and total N concentration of the flag leaves (N-Flag) and ears (N-Ear)Nine genotypes and three replicates per genotype were considered, accounting for a total of 54 values under RF (water stress) conditions, including fertilized and nonfertilized conditions and under fertilized conditions (HN), including the two water conditions. For the $\delta^{18}O$ and δ^2H of DM (flag leaves, ears, and roots), only two cultivars and two landraces were considered (24 plots). Analyses were performed on samples from the 2010 crop season. Level of significance: not significant, ns, $P > 0.05$; ***, $P < 0.001$; **, $P < 0.01$; *, $P < 0.05$.

Isotope/Organ/ Fraction	g_s				*GY*				*N-Flag*				N-Ear			
	SI	***RF***	***HN***	***LN***	***SI***	***RF***	***HN***	***LN***	***SI***	***RF***	***HN***	***LN***	SI	RF	HN	LN
Hydrogen																
δ^2H_{roots} DM	0.2ns	0.2ns	0.4ns	0.4ns	−0.2ns	−0.1ns	0.2ns	0.4ns	−0.1ns	−0.1ns	0.5*	−0.1ns	−0.2ns	−0.2ns	0.5*	−0.1ns
$\delta^2H_{stem\ water}$	−0.3*	0.4**	−0.1ns	0.1ns	−0.3ns	−0.1ns	−0.2ns	0.1ns	−0.1*	0.3*	−0.2ns	−0.1ns	0.2ns	0.1ns	0.3*	−0.0ns
δ^2H_{flag} DM	−0.2ns	−0.7***	−0.8***	−0.3ns	0.1ns	−0.5*	−0.6**	−0.3ns	0.3ns	0.5*	−0.6**	0.0ns	0.3ns	0.7***	−0.1ns	0.1ns
δ^2H_{flag} WSF	−0.2*	−0.6**	−0.4**	−0.1ns	−0.1ns	−0.3*	−0.4**	−0.1ns	−0.1*	0.6**	−0.4**	0.2ns	0.1ns	0.7***	0.2ns	0.2ns
δ^2H_{ear} DM	−0.2ns	−0.4**	−0.8***	−0.4ns	0.3ns	−0.4*	−0.6**	−0.4ns	0.5ns	0.4**	−0.3ns	0.4ns	0.5*	0.9***	0.2ns	0.5*
δ^2H_{ear} WSF	0.2ns	−0.6***	−0.4**	−0.3*	0.4**	−0.5***	−0.3*	−0.3*	0.4ns	0.7***	−0.1ns	0.1ns	0.3*	0.5***	0.1ns	0.1ns
δ^2H_{grain}	0.1ns	−0.6***	−0.5***	−0.5***	0.3*	−0.4**	−0.5***	−0.5***	0.7ns	0.4**	−0.5***	0.1ns	0.6***	0.4**	−0.2ns	−0.0ns
Oxygen																
$\delta^{18}O_{roots}$ DM	0.1ns	−0.1ns	0.1ns	0.3ns	0.1ns	−0.2ns	0.1ns	0.3ns	0.5ns	−0.1ns	−0.1ns	−0.0ns	−0.3ns	0.1ns	−0.1ns	−0.0ns
$\delta^{18}O_{xylem\ water}$	0.3*	0.3*	0.3*	−0.0ns	0.3ns	−0.2ns	−0.3*	0.1ns	−0.2*	−0.3*	−0.2ns	−0.1ns	0.2ns	0.2ns	0.4**	0.1ns
$\delta^{18}O_{flag}$ DM	0.1ns	−0.2ns	−0.4**	−0.3ns	0.1ns	−0.2ns	−0.3*	−0.3ns	−0.2ns	0.0ns	−0.5***	−0.1ns	−0.1ns	0.2ns	−0.2ns	0.2ns
$\delta^{18}O_{flag}$ WSF	−0.3*	0.0ns	−0.8***	−0.2ns	−0.2ns	−0.5**	−0.6***	−0.2ns	−0.7*	−0.3ns	−0.5***	−0.1ns	−0.6***	−0.2ns	−0.3*	0.1ns
$\delta^{18}O_{ear}$ DM	−0.1ns	0.2ns	−0.2ns	0.1ns	0.1ns	−0.3ns	−0.1ns	0.1ns	−0.1ns	−0.1ns	0.1ns	−0.2ns	−0.0ns	−0.0ns	−0.0ns	−0.1ns
$\delta^{18}O_{ear}$ WSF	−0.1ns	0.2ns	−0.3*	−0.3*	0.1ns	−0.4**	−0.1ns	−0.3*	−0.1ns	−0.2ns	−0.1ns	−0.1ns	−0.2ns	−0.1ns	−0.1ns	−0.1ns
$\delta^{18}O_{grain}$	0.1ns	0.1ns	−0.0ns	−0.0ns	−0.2ns	−0.2ns	−0.2ns	0.1ns	−0.2ns	−0.2ns	−0.1ns	0.1ns	−0.3*	−0.2ns	−0.1ns	−0.2ns
Carbon																
$\delta^{13}C_{flag}$ DM	−0.2ns	−0.7***	−0.7***	−0.59***	0.1ns	−0.3*	−0.6***	−0.6***	0.4s	0.3*	−0.6***	0.1ns	0. 5***	0.4**	−0.1ns	0.1ns
$\delta^{13}C_{flag}$ WSF	−0.4**	−0.4**	−0.8***	−0.6***	−0.3ns	−0.3*	−0.6***	−0.6***	−0.5**	0.1ns	−0.6***	−0.1ns	−0.4**	0.2ns	−0.1ns	0.1ns
$\delta^{13}C_{ear}$ DM	−0.1ns	−0.5***	−0. 7***	−0.5***	0.4**	−0.4**	−0.4**	−0.5***	0.5ns	0.4**	−0.3*	0.1ns	0.5***	0.4**	−0.1ns	0.2ns
$\delta^{13}C_{ear}$ WSF	−0.1ns	−0.3*	−0.6***	−0.42**	0.4**	−0.5***	−0.4**	−0.4**	0.4ns	0.3*	−0.2ns	0.1ns	0.2ns	0.3*	−0.1ns	0.2ns
$\delta^{13}C_{grain}$	−0. 4**	−0.7***	−0.8***	−0.29*	−0.3*	−0.3*	−0.8***	−0.3*	0.21**	0.47***	−0.57***	0.3*	0.16ns	0.4**	−0.3*	0.3ns

Table 5. *Stepwise analysis between GY, and $\delta^{13}C$, $\delta^{18}O$, and $\delta^{2}H$ isotope compositions*

Stepwise analysis for the whole set of nine genotypes per three replicates in 2010, under SI, RF, N fertilization (HN), and without N fertilization (LN), including all growing conditions (global) and a combination of SI and N fertilization (SI + HN), SI without N fertilization (SI-LN), RF conditions and N fertilization (RF + HN), and RF conditions without N fertilization (RF-LN), with *GY* as a dependent variable, and $\delta^{13}C$, $\delta^{18}O$, and $\delta^{2}H$ isotope composition of mature kernels (grains), soluble organic matter of flag leaves (leaf WSF), and ears (ear WSF), and oxygen and hydrogen isotope composition of stem water (stem W) as independent variables. The "global" stepwise analysis represents values obtained from the average of the three replicates per genotype under each growing condition (108 plots, $n = 36$). The "SI" and "RF" stepwise analyses represent values obtained from the average of three replicates per genotype, including HN and LN conditions ($n = 18$). The "HN" and "LN" stepwise analyses represent values obtained from the average of three replicates per genotype, including SI and RF conditions ($n = 18$).

Treatment	Variable Chosen	*r*	R^2	Significance
Global	$\delta^{13}C_{grain}$	0.71	0.51	0.000
	$\delta^{13}C_{grain}$, $\delta^{18}O_{flag}$ WSF	0.83	0.70	0.000
	$\delta^{13}C_{grain}$, $\delta^{18}O_{flag}$ WSF, $\delta^{13}C_{flag}$ WSF	0.87	0.75	0.000
	$\delta^{13}C_{grain}$, $\delta^{18}O_{flag}$ WSF, $\delta^{13}C_{flag}$ WSF, $\delta^{13}C_{ear}$ WSF	0.89	0.80	0.000
SI	$\delta^{2}H_{ear}$ WSF	0.75	0.57	0.000
	$\delta^{2}H_{ear}$ WSF, $\delta^{2}H_{stem\ W}$	0.85	0.71	0.000
RF	$\delta^{2}H_{grain}$	0.61	0.38	0.006
	$\delta^{2}H_{grain}$, $\delta^{18}O_{flag}$ WSF	0.84	0.70	0.000
HN	$\delta^{13}C_{grain}$	0.89	0.80	0.000
	$\delta^{13}C_{grain}$, $\delta^{18}O_{flag}$ WSF	0.94	0.82	0.000
	$\delta^{13}C_{grain}$, $\delta^{18}O_{flag}$ WSF, $\delta^{18}O_{grain}$	0.96	0.92	0.000
LN	$\delta^{18}O_{flag}$ WSF	0.76	0.58	0.000
	$\delta^{18}O_{flag}$ WSF, $\delta^{13}C_{grain}$	0.84	0.70	0.000

reduction in the C_i/C_a ratio, due to either an increase in photosynthetic capacity or a decrease in g_s (Farquhar and Richards, 1984; Condon et al., 2004). Such findings agree with our results, where fertilized plots showed lower g_s compared with that of nonfertilized plots (Table 1). Moreover, the higher $\delta^{2}H$ values in the leaf DM under N fertilization can be explained by the evaporative ^{2}H enrichment of leaf water. In the modified Péclet effect model (Farquhar and Lloyd, 1993), transpiration has been observed to reduce ^{2}H-enrichment of leaf water due to a mixture of leaf water and source of water (Cernusak et al., 2016). Therefore, the increase in $\delta^{2}H$ in the leaf DM under N fertilization observed in our experiments can be explained by reduced g_s and a subsequent decrease in transpiration resulting in a decreased Péclet effect (Cernusak et al., 2016). In addition, $\delta^{13}C$ and $\delta^{2}H$ were positively correlated with N-Flag (nitrogen content of the flag leaves DM) and negatively correlated with g_s under RF and SI conditions (both including HN and LN treatments; Table 4). Such results indicate that biomass is increased with increases in nitrogen supply, forcing the plants to compete for water resources and exacerbating water stress (therefore resulting in lower g_s and higher $\delta^{13}C$ and $\delta^{2}H$). However, under SI conditions, N fertilization (which may have increased growth and consequently biomass and yield) did not increase N-Flag as a consequence of a growth dilution effect in the leaf due to leaf expansion (Salazar-Tortosa et al., 2018). This result is supported by the negative correlation between *GY* and N-Flag ($r = -0.426$, $P < 0.01$, data not shown) under SI conditions, whereas under RF conditions the correlation was positive ($r = 0.285$, $P < 0.05$, data not shown). Thus, N fertilization under SI conditions showed positive correlation between $\delta^{13}C$ and $\delta^{2}H$ and N-Flag, supporting the idea that plants with lower N-Flag showed higher *GY* (i.e. biomass), which, as mentioned before, may have caused a temporary mild water stress during plant growth.

However, under HN conditions (but including the two water regimes), correlations of $\delta^{13}C$ and $\delta^{2}H$ with N-Flag were in some cases negative (Table 4). These results suggest that under HN conditions (including SI and RF regimes), N fertilization does not necessarily have a negative effect as water stress increases, but rather, the opposite is observed. It has been reported that providing N when there is water available in the soil (i.e. under irrigation conditions) may improve not only growth but also the water status of the crop by contributing to better root growth (Jensen et al., 1990). Overall, these findings suggest that $\delta^{2}H$ and $\delta^{13}C$ are subject, at least in part, to a similar source of variation; meaning that both isotopes responded with an increase in isotope signature as a result of N fertilization for a given level of water regime (SI, RF) or with a decrease in isotope signature in response to water supply under nitrogen fertilization conditions (HN).

Differences in $\delta^{13}C$, $\delta^{18}O$, and $\delta^{2}H$ between Cultivars and Landraces

GY was higher in cultivars compared with that in landraces for both growing years of the study. Although landraces in this study were chosen on the basis of their close phenology to modern cultivars, the latter

on average still reached heading 5 d earlier (data not shown). Cultivars have been observed as having a shorter duration to heading compared with landraces (Araus et al., 2002, 2013), escaping from water stress produced during the reproductive stage (Araus et al., 2007). In fact, more enriched values of $\delta^{13}C$, δ^2H, and $\delta^{18}O$ in grains were observed in landraces compared with that in cultivars (Table 1), evidencing that landraces were exposed to an extended stress episode contributing to a lower *GY* compared with cultivars (Araus et al., 2007, 2013).

Applicability of $\delta^{13}C$ and $\delta^{18}O$ for Assessing Plant Performance

In agreement with previous studies (Condon et al., 1987; Araus et al., 1998, 2003; Fischer et al., 1998; Monneveux et al., 2005; Lopes and Reynolds, 2010), $\delta^{13}C$ was negatively correlated with *GY* when all growing conditions were combined (Fig. 4). Conversely, some correlations of $\delta^{13}C$ with *GY* under SI conditions (including HN and LN conditions) were positive for the flag leaves and the ears, and negative for the grains (Table 4). The positive slope between $\delta^{13}C$ (in the flag leaves and ear) and *GY* under SI may be the consequence of N fertilization causing water stress, as discussed previously. Moreover, negative genotypic correlations with *GY* were only observed with $\delta^{13}C_{grain}$ (Supplemental Table S2) and were weaker in 2010 than in 2011. Indeed, correlations between *GY* and $\delta^{13}C_{grain}$ decreased under poor growing conditions (Supplemental Fig. S1), whereas the $\delta^{18}O_{flag}$ WSF showed the opposite trend (Supplemental Fig. S1). According to our results, in trials under drought conditions with mean yields below 2 $Mg \cdot ha^{-1}$ (as was the case for 2010), nonsignificant (Araus et al., 2003) or even positive relationships between *GY* and $\delta^{13}C_{grain}$ (Voltas et al., 1999) have been reported, suggesting that higher plant water-use efficiency (and thus higher $\delta^{13}C$) increases yield under stress (Farquhar and Richards, 1984; Araus et al., 2003, 2013; Condon et al., 2004). Thus, $\delta^{13}C_{grain}$ could be a good indicator of the water strategy that plants are following.

Concerning $\delta^{18}O$ in 2011, the isotope composition in the grain ($\delta^{18}O_{grain}$) was strongly associated with *GY* ($r = -0.83$, $P < 0.000$) under all water regimes and nitrogen levels combined (Table 3). However, the correlation was weaker in 2010 ($r = -0.21$, $P = 0.027$, Fig. 4). The lack of consistency between the 2010 and 2011 crop seasons may be related to differences in environmental conditions. *GY* was much lower in 2010 (1.7 $Mg \cdot ha^{-1}$ on average) compared with that in 2011 (3.1 $Mg \cdot ha^{-1}$ on average). In fact, in a study on wheat by Barbour et al. (2000), correlations of $\delta^{18}O_{grain}$ with *GY* and g_s were also not constant among the three seasons they analyzed. In the same study, $\delta^{18}O_{grain}$ was only correlated with *GY* during one season, and it was the season with the highest precipitation and lowest solar radiation. Such results indicate that $\delta^{18}O_{grain}$ might not reflect evaporative conditions under narrow environmental ranges and with moderate to severe drought. Therefore, as a consequence of high levels of remobilization under more severe water conditions, preservation of evaporative conditions imprinted in the $\delta^{18}O$ of grains might be low or even nonexistent (Barbour et al., 2000; Ferrio et al., 2007). Likewise, the disparity observed in our study between the two growing seasons regarding the relationship between $\delta^{18}O_{grain}$ and *GY* could be due to the relative proportions of remobilized photo-assimilates (Barbour et al., 2000). Triose phosphates formed from photosynthesis during the day are converted to Suc for transport (Barbour and Farquhar, 2000). Thus, the main exchange of water with carbonyl oxygen occurs in the leaves during the formation of triose phosphate molecules, because two of the three oxygen atoms present in the molecule belong to carbonyl groups (Sternberg et al., 1986; Barbour et al., 2000). Indeed, correlations of *GY* with $\delta^{18}O_{flag}$ in the WSF and DM were higher than with $\delta^{18}O_{grain}$ (Fig. 4; Supplemental Fig. S2), indicating that signals of the evaporative conditions are still preserved in leaf assimilates but not in other organs because no correlations of *GY* with the $\delta^{18}O_{ear}$ (either DM or WSF), $\delta^{18}O_{grain}$, or $\delta^{18}O_{roots}$ were observed. On one hand, as mentioned previously, such a lack of correlation may be related to the $\delta^{18}O$ fractionation associated with biochemical reactions during the synthesis of organic matter (Farquhar and Lloyd, 1993) and its subsequent transport (Offermann et al., 2011). On the other hand, the $\delta^{18}O$ of organic matter may also be influenced by the source of water (Figs. 1 and 2; Epstein et al., 1977; Yakir et al., 1990b; Roden et al., 2000; Williams et al., 2005; Barbour, 2007). This is not straightforward because the $\delta^{18}O$ of source water (water from the base of the stem) is also subjected to evaporative enrichment in the leaf during transpiration (Farquhar and Lloyd, 1993) and during grain formation (Fig. 2; Pande et al., 1994). In fact, it has been reported that the $\delta^{18}O$ of water in developing grains exhibits a biphasic enrichment compared with stem water (Pande et al., 1994). The biphasic enrichment may be linked to developmental metabolism of the grain and rapid loss of water, together with oxidative metabolism during later stages of maturation (Pande et al., 1995). Such biphasic enrichment in the grains could therefore affect $\delta^{18}O$, which consequently might have enriched the $\delta^{18}O$ of water from the developing grains compared with that in stem water (Table 2). Accordingly, the enrichment of water in the grain could be an additional factor that may hinder the registration of environmental conditions in the $\delta^{18}O_{grain}$ DM. Moreover, the $\delta^{18}O$ of water in the flag leaves was enriched compared with that in water from developing grains and stems (Fig. 2; Table 2), an idea that also agrees with the widely reported strong evaporation processes taking place in the leaf (Farquhar and Gan, 2003; Barbour et al., 2004). Besides, the $\delta^{18}O$ from the water of photosynthetic and transpiring organs such as the flag leaves was strongly correlated with *GY* (Table 3) when all growing conditions were

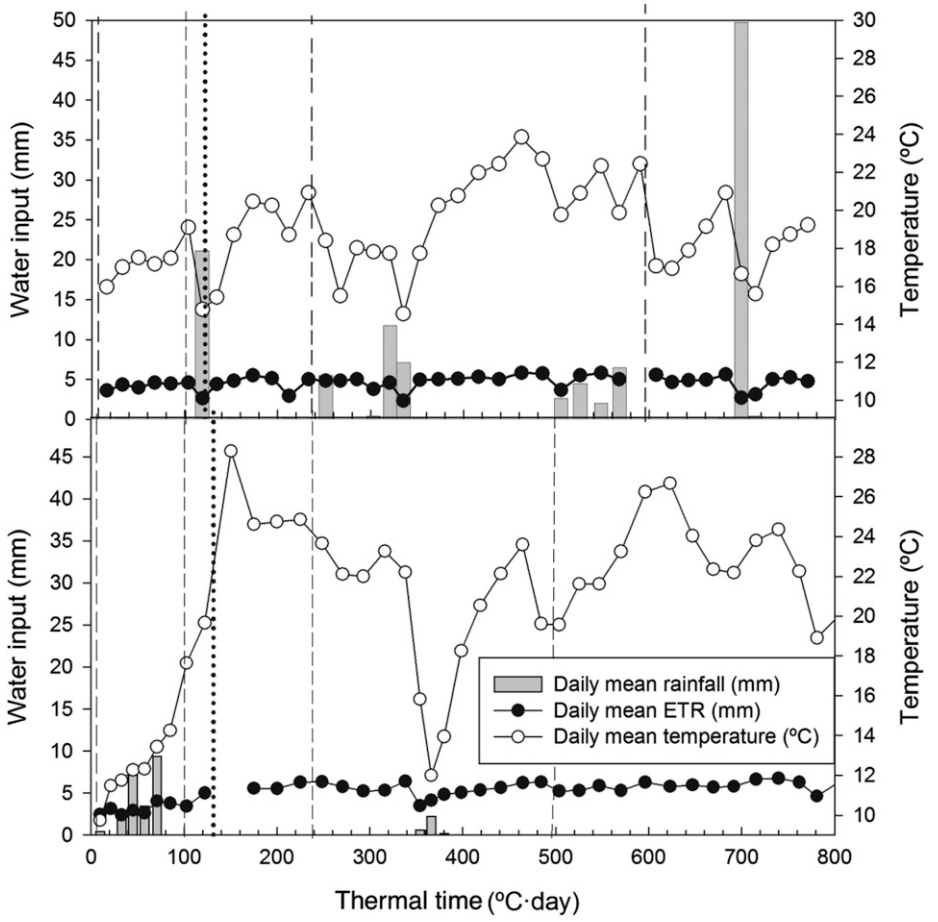

Figure 5. Daily mean precipitation (mm), evapotranspiration (mm), and air temperature (°C) during the growing season from flowering to physiological maturity expressed as thermal time (°C·day) during the 2010 (top panel) and 2011 crop seasons (bottom panel). ETR = electron transport rate. Vertical dashed lines = dates of irrigation. Vertical dotted lines = sampling dates.

included. In short, the strong correlation between *GY* and $\delta^{18}O$ from water in leaves suggests that leaf water mainly reflects evaporative enrichment and thus environmental conditions, with the additional advantage (at least in the case of $\delta^{18}O$) of avoiding the fractionation associated with biochemical reactions during the synthesis of organic matter (Farquhar and Lloyd, 1993).

Applicability of Plant δ^2H to Assess Plant Performance

Strong correlations between $\delta^{18}O$ and δ^2H in the cellulose of leaves have been reported in the literature, which suggests similar sources of variation for plant isotopic signals (Epstein et al., 1977), whereas the absence of a correlation would indicate additional biochemical effects (Sternberg et al., 1986). Keeping this in mind, in the 2010 season, the absence of significant correlations between $\delta^{18}O_{grain}$ and δ^2H_{grain} (Fig. 3), together with the lack of any relationship between $\delta^{18}O_{grain}$ and *GY*, suggests that $\delta^{18}O_{grain}$ is more sensitive to biochemical reactions than δ^2H_{grain} during grain formation (Farquhar and Lloyd, 1993) or is more likely to undergo exchange with the (^{18}O) of source water (Barbour, 2007).

Although exchange of hydrogen isotopes with water within the cytosol can affect the δ^2H of organic compounds and the contribution to NADPH (Zhou et al., 2018), the analysis of δ^2H depletion in plant organs could be used as an indicator of the net isotopic effect associated with NADPH synthesis in the chloroplast (Hayes, 2001; Zhou et al., 2010). Therefore, if NADPH is not regenerated continuously, reduction power can be strictly limited, and distinct metabolic processes such as photosynthetic electron transport or nitrate reduction (Bloom, 2015) may inhibit carbon fixation (Foyer et al., 2012). In agreement with our results (Fig. 3), data from a study in mature kernels of wheat (Liu et al., 2015) also showed a strong positive correlation between $\delta^{13}C$ and δ^2H, supporting the idea that both isotopes's composition (even in heterotrophic organs) are affected by photosynthetic activity even if the source of variation is different. Thus, for example, whereas a decrease in photosynthetic activity caused by water stress is the consequence of a lower CO_2 availability (which increases $\delta^{13}C$), the decreased activity diminishes the synthesis of NADPH produced in the chloroplast (and then δ^2H decreases less).

However, as discussed previously for $\delta^{18}O$, the δ^2H of organic matter may also be affected by the source water δ^2H (Fig. 2) and be subjected to evaporative enrichment in the leaves and to biphasic enrichment in grains. Nevertheless, in spite of these fractionation processes, there were good correlations of the δ^2H from

the flag leaves, ears, and grains with g_s and *GY* (Fig. 4). In fact, the only isotope composition that correlated with *GY* (as a dependent variable) in the stepwise analysis in 2010 was the δ^2H under SI and RF conditions (SI $r = 0.75$, $P = 0.000$; RF $r = 0.62$, $P = 0.006$). In contrast to δ^{18}O, these results suggest that δ^2H was not hindered by fractionation processes within different organs, either during transport of assimilates to the grains or during heterotrophic metabolism within the grains. Therefore, δ^2H may provide simultaneous time-integrated records of the photosynthetic and evaporative performance of the plant during crop development based on, among other aspects, its tighter association with $\delta\ ^{13}$C than with $\delta\ ^{18}$O.

CONCLUSIONS

In autotrophic organs, such as the flag leaf, δ^2H was not only affected by changes in transpiration and g_s but also by photosynthetic carbon metabolism because the net isotopic effect (δ^2H depletion) was negatively associated with ETR. Contrastingly, δ^2H enrichment in heterotrophic organs such as the grains and roots was associated with postphotosynthetic effects because there are several processes that lead to ^{2}H-enrichment of carbohydrates. In the case of the ears, their intermediate δ^2H values (lying between the flag leaves and grains) may be the consequence of different factors—such as lower transpiration compared with that in the leaves, the mixotrophic nature of the bracts, or some degree of CAM metabolism.

The significant correlations between δ^2H and GY and the existence of genotypic variability in plant δ^2H are encouraging when considering this isotope for assessing plant performance under different growing conditions.

MATERIALS AND METHODS

Germplasm Used and Experimental Conditions

Ten durum wheat (*Triticum turgidum* ssp *durum* [Desf.] Husn.) genotypes were sown: five historical Spanish landraces (*Blanqueta, Griego de Baleares, Negro, Jerez 37,* and *Forment de Artes*) and five modern Spanish commercial varieties released after 1990 (*Anton, Bolo, Don Pedro, Regallo,* and *Sula*). Landraces were chosen based on their similarity to the phenology of modern cultivars. Field experiments were conducted during the 2010 and 2011 growing seasons at the experimental station of the Instituto Nacional de Investigación y Tecnología Agraria y Alimentaria (INIA) of Aranjuez (40°03′N, 3°31′E, 500 m asl), with experimental conditions explained in Sanchez-Bragado et al. (2014). Two water treatments (SI and RF) combined with two nitrogen regimes (fertilized, HN; and nonfertilized, LN) were assayed. The trials were planted on December 30, 2010 and November 18, 2011 in plots with six rows 0.20 m apart, covering a total area of 6 m^2 (5 m length and 1.2 m width) per plot. Total accumulated precipitation during the 2010 and 2011 seasons was 275.4 and 126.1 mm, respectively. For both years, sprinkler irrigation was applied to irrigated plots around GS41 (beginning of April; Zadoks et al., 1974) and GS71 (around May 15th and 30th) with approximately 60 mm supplied on each date. Environmental conditions during growth are detailed in Figure 5. Prior to sowing, all trials received 60 kg ha^{-1} of phosphorous as superphosphate (18%), and 60 kg ha^{-1} potassium as potassium chloride (60%). Further, the HN plants were dressed with nitrogen applied at the beginning of tillering (January 27th in 2010 and December 29th in 2011) and jointing (March 20th in 2010 and February 20th in 2011) using a dose of 45 kg ha^{-1} and 105 kg ha^{-1} of urea (46%), respectively. The LN plants were not N fertilized, relying exclusively on the N available in the soil before sowing. Water and nitrogen treatments were arranged according to a split-split plot design with three replicates. Experimental plots were kept free of weeds, insects, pests, and diseases by recommended chemical measures (Sanchez-Bragado et al., 2014).

Sampling was performed around 7 d after anthesis, corresponding to the GS71-75 Zadoks stages (Zadoks et al., 1974) in 2010 and two weeks after anthesis (stages GS75-81) in 2011. In 2010, the genotype *Foment de Artes* was discarded due to late phenology. Also in 2011, all five landraces under SI were discarded due to lodging. In 2010, roots were collected from the upper layer (0–10cm) with a split tube sampler (Ref. 04.17.01.C, Eijkelkamp Soil & Water), rinsed with distilled water, and then placed inside a paper envelope. Thereafter, five representative flag leaves and ears were collected per plot, then oven dried together with collected roots at 70°C for 48 h, then weighed and finely ground for hydrogen, oxygen, and carbon isotope analyses (in total DM). In 2011, flag leaves and developing grains from five representative tillers were collected and immediately frozen for subsequent water extraction. Stomatal conductance (g_s) was measured with a leaf porometer (Decagon; http://www.decagon.com) in one leaf per plot. At maturity, the central four rows of each plot were harvested and the *GY* was recorded. Subsequently, mature kernels were processed for isotope analysis. Harvest was performed manually and by machine in 2010 and 2011, respectively.

Carbon Isotope Analyses

Carbon isotope analyses of mature grains as well as the total DM and WSF of the flag leaf blades and ears from the field trials, together with the DM of the flag leaves from the growth chamber experiment, were performed using an Elemental Analyzer (EA; Flash 1112 EA, Thermo Fisher Scientific) coupled with an isotope ratio-mass spectrometer (IRMS; Delta C IRMS, Thermo Fisher Scientific) operating in continuous flow mode in order to determine the stable carbon (^{13}C/^{12}C) isotope ratios of the same samples. Samples of approximately 1 mg of total DM for mature grains, 0.7 mg for flag leaves and ears, and reference materials were weighed into tin capsules, sealed, and then loaded into an automatic sampler (Thermo Fisher Scientific) before EA-IRMS analysis. The ^{13}C/^{12}C ratios of plant material were expressed in δ notation (Coplen, 1988): $\delta^{13}C = (^{13}C/^{12}C)_{sample} / (^{13}C/^{12}C)_{standard} - 1$. "Sample" refers to plant material and "standard" to international secondary standards of known ^{13}C/^{12}C ratios [International Atomic Energy Agency (IAEA) CH7 polyethylene foil, IAEA CH6 Suc, and United States Geological Survey (USGS) 40 l-Glu] calibrated against Vienna Pee Dee Belemnite calcium carbonate with an analytical precision (SD) of 0.10‰.

Measurements were carried out at the Scientific Facilities of the University of Barcelona. The δ^{13}C of flag leaves (DM), ears (DM), roots, and mature kernels are referred to as $\delta^{13}C_{flag}$ DM, $\delta^{13}C_{ear}$ DM, $\delta^{13}C_{roots}$ DM, and $\delta^{13}C_{grain}$, respectively.

Oxygen Isotope Analyses

The ^{18}O/^{16}O ratios of the same mature grains (as well as the total DM and WSF of flag leaf blades and ears) were determined by an online pyrolysis technique using a Thermo-Chemical Elemental Analyzer (TC/EA; Thermo Fisher Scientific) coupled with an IRMS (Delta C Finnigan MAT). Samples of 1 mg of total DM for mature grains, flag leaves, ears, roots, and reference materials were weighed into silver capsules, sealed, and oven-dried at 60°C for no less than 72 h to remove moisture, and then loaded into an automatic sampler. Results were expressed as δ^{18}O values, using two secondary standards (IAEA 601 and IAEA 602) calibrated against Vienna Standard Mean Oceanic Water (VSMOW), and the analytical precision was ~0.25‰. Analyses were conducted at Iso-Analytical Limited (Crewe). The δ^{18}O of flag leaves (DM), ears (DM), roots, and mature kernels are referred to as $\delta^{18}O_{flag}$ DM, $\delta 18O_{ear}$ DM, $\delta 18O_{roots}$ DM, and $\delta^{18}O_{grain}$, respectively.

Hydrogen Isotope Analyses

The ^{2}H/^{1}H ratios of the same mature grains, as well as the total DM and WSF of the flag leaf blades and ears (and only leaves DM in the growing chamber experiment) were determined by an online pyrolysis technique using a TC/EA (Thermo Fisher Scientific) coupled with an IRMS (Delta plus xp). Samples of 0.15 mg of total DM for mature grains, flag leaves, ears, roots, and

reference materials were weighed into silver capsules, sealed, and oven-dried at 60°C for not less than 72 h to remove moisture, and then loaded into an automatic sampler. In addition, samples were always kept under free moisture conditions with silica gel in a desiccator. Results were expressed as δ^2H values, using international secondary standards (for calibration and checking precision and accuracy) of known ^{2}H/^{1}H ratios (IAEA CH7 polyethylene foil, 5α-androstane, coumarin, and eicosanoic acid methyl ester) calibrated against VSMOW, and the analytical precision was ~0.5‰. In addition, a secondary internal standard (IAEA 601, δ^2H = −85.1‰) was selected to provide at least a two-point calibration (normalization) of the hydrogen isotope delta scale anchored by VSMOW. Measurements were carried out at the Scientific Facilities of the University of Barcelona. The δ^2H of flag leaves (DM), ears (DM), roots, and mature kernels are referred to as $\delta 2H_{flag}$ DM, $\delta 2H_{ear}$ DM, $\delta 2H_{roots}$ DM, and δ^2H_{grain}, respectively.

Water-Soluble Fraction

The protein-free WSFs of the flag leaves and ears were extracted from the same dry samples tested for carbon, hydrogen, and oxygen isotopes, as described previously in Cabrera-Bosquet et al. (2011) and Yousfi et al. (2013). Aliquots of 40 μL (carbon), 20 μL (hydrogen), and 100 μL (oxygen) of supernatant containing protein-free WSF were transferred into tin capsules for carbon analysis, and into silver capsules for hydrogen and oxygen analyses. The capsules containing the aliquots were oven dried at 60°C. The WSFs of the δ^{13}C, δ^2H, and δ^{18}O of flag leaves and ears are referred to as $\delta^{13}C_{flag}$ WSF, $\delta 13C_{ear}$ WSF, $\delta 2H_{flag}$ WSF, $\delta 2H_{ear}$ WSF, $\delta 18O_{flag}$ WSF, and $\delta 18O_{ear}$ WSF, respectively. Additionally, in order to estimate any possible exchange between the samples and the water used to extract the protein-free WSF, the powdered samples were suspended using three water reference sources with different δ^2H (snow water, δ^2H = −77.5‰; deuterated water, δ^2H = −94.4‰, and seawater, δ^2H = −3.3‰). In fact, using extraction water sources with different δ^2H signatures does not significantly affect the δ^2H of the soluble fraction, and the absolute differences in δ^2H between soluble fractions extracted from the DM with the different water sources were minor (Supplemental Table S3).

Hydrogen and Oxygen Composition in Plant Water

To determine source water variations in the 2010 and 2011 field experiments, a portion of the stem base was harvested in the field. In 2010, variations in source water were determined from pressed stem juice. Stem base segments were pressed with a high-pressure press in order to obtain a liquid extract. Subsequently, extracted liquid was transferred to 2-mL glass vials with crimp caps. Glass vials were sealed and sterilized in a water bath at 100°C for 2 h to prevent fermentation processes, and then kept cool until isotope analysis. In 2011, a portion of the stem base was placed into sealed tubes immediately after sampling and subsequently frozen in a freezer at −20°C. Thereafter, water was extracted from the stem base using a cryogenic vacuum distillation line (Dawson and Ehleringer, 1993). The δ^2H and δ^{18}O of water extracted from the stem are referred to as $\delta^2H_{stem\ W}$ and $\delta^{18}O_{stem\ W}$, respectively.

In 2011, flag leaves and developing grains were collected and placed into sealed tubes and then frozen immediately after sampling. Thereafter, water was extracted from the developing grains and flag leaves using a cryogenic vacuum distillation line (Dawson and Ehleringer, 1993) and measured together with stem water samples. The δ^2H and δ^{18}O of water extracted from flag leaves and developing grains are referred to as $\delta^2H_{flag\ W}$, $\delta\ ^2H_{grain\ W}$, $\delta^{18}O_{flag\ W}$, and $\delta^{18}O_{grain\ W}$, respectively.

Oxygen and hydrogen compositions (δ^{18}O, δ^2H) in water distilled from stem bases, flag leaves, and developing grains (experiment 2011) and stem juice extracts (stem water, experiment 2010) were determined by laser spectroscopy at the Serveis Científico-Tècnics of the Universitat de Lleida using a Picarro L2120i (Picarro, Inc.) coupled to a high-precision vaporizer A0211. All samples were centrifuged at 12,000 *g* in order to remove any suspended solid, and the supernatants were transferred to glass vials with a 250-mL insert. In the case of stem juice, because large amounts of sugars reduce the performance of the vaporizer, juice samples were diluted to 50% with distilled water of known isotopic composition prior to injection as explained in Sánchez-Bragado et al. (2016). At the same time, the potential presence of organic contaminants was checked using the postprocessing software ChemCorrect 1.2.0 (Picarro), giving in some cases positive results. Consequently, the data were thereafter corrected for consistency across all samples (to avoid undesired effects of organic contaminants) as described by Martín-Gómez et al. (2015). Nevertheless, we found very strong correlations between corrected and uncorrected values (r^2 = 0.998 for δ^{18}O; r^2 = 0.992 for δ^2H; n = 106), with 83% of the samples showing differences lower than 0.4‰ for δ^{18}O, and lower than 4‰ for δ^2H.

Isotopes were expressed in delta (δ) notation (‰) relative to VSMOW (i.e. isotopic composition of oxygen, δ^{18}O, and hydrogen, δ^2H). Raw values were calibrated against three internal laboratory references [calibrated against IAEA standards VSMOW2, Standard Light Antarctic Precipitation2 (SLAP2), and Greenland Ice Sheet Precipitation]. Overall uncertainty, determined as the SE of repeated analyses, (n = 20) of a reference material not included in the calibration, was 0.05‰ and 0.17‰, for δ^{18}O and δ^2H, respectively.

Dual-Water Equilibration Method to Quantify the Fraction of Exchangeable H

A dual-water equilibration method was performed in order to quantify the fraction of exchangeable H and to determine the δ^2H in the nonexchangeable H fraction (Schimmelmann et al., 2001; Sauer et al., 2009; Qi and Coplen, 2011). Dry leaf material and the WSF of the same sample, plus standards, were used for the dual-water equilibration method. A set of three aliquots extracted from the same sample plus the standards were weighed and loaded into individual silver capsules, and then each capsule was held in a plastic tray. Each plastic tray was placed in a glass desiccator for equilibration with water sources with different δ^2H. One set was equilibrated in a glass desiccator with water depleted in ^{2}H (ambient snow water, δ^2H = −77.5‰), and the second set was equilibrated with seawater (ambient seawater, δ^2H = −3.3‰). In each glass desiccator, a set of standards was also included. Samples were equilibrated in each desiccator for 7 d at ambient temperature (25°C). In order to remove the moisture prior the equilibration period, the desiccators were purged with helium for 5 minutes at 120 mL min^{-1}. Subsequently, samples from light and heavy water were dried in separate desiccators filled with Sicapent (P_2O_5) for at least 7 d. In parallel, a set of identical samples used for water equilibration was oven dried at 50°C for 7 d. After 7 d of oven and Sicapent drying, δ^2H measurements were performed with an online pyrolysis technique using a TC/EA (Thermo Fisher Scientific) coupled with an IRMS (Delta plus xp) as described previously. In addition, the samples in the TC/EA carousel were purged with helium (120 mL min^{-1}). The helium purged gas was fed from the top of the TC/EA reactor. All results were normalized to the VSMOW-SLAP isotope scale (Coplen, 1988) using the Laboratory Information Management System for Light Stable Isotope, so that the δ^2H VSMOW of SLAP was −428‰ relative to VSMOW (Gonfiantini, 1978). Results were expressed as δ^2H values, using the same international secondary standards of known ^{2}H/^{1}H ratios indicated before, and the analytical precision was ~0.5‰. Finally, the fraction of total hydrogen that is exchangeable (f_e) was calculated as described by Schimmelmann et al. (2001):

$$f_e = (\delta^2H_{TA} - \delta^2H_{TB}) / (\delta^2H_{WA} - \delta^2H_{WB})$$

where δ^2H_{TA} and δ^2H_{TB} are the δ^2H values of the total hydrogen of the same samples equilibrated with water standards wA and wB, respectively; and where δ^2H_{WA} and δ^2H_{WB} are the δ^2H values of water vapor A and B, respectively. Then the isotopic composition of nonexchangeable hydrogens (δ^2H_n) can be calculated as follows:

$$\delta^2H_n = (\delta^2H_{TA} - f_e(\delta^2H_{WA} - \varepsilon))/(1 - f_e)$$

where ε is the fractionation effect between exchangeable organic hydrogen and water hydrogen. Although ε might range from 30% to 110%, depending on the molecule structure containing organic exchangeable H (Schimmelmann, 1991), typical values for most material of interest in environmental studies (proteins, cellulose, humic acids) presented a fractionation effect of 80‰ ± 20‰ (Wassenaar and Hobson, 2000). Therefore the ε factor used in the calculation was 80‰, as has been previously determined experimentally for well-defined cellulose (Schimmelmann, 1991). Then the true δ^2H_n values of the WSF and DM were calculated (Supplemental Table S4); and the δ^2H of the WSF and DM in the flag leaves, the ears, and the grains were corrected using the fraction of total hydrogen that is exchangeable, obtained within the different equilibration conditions. Thus the δ^2H of the WSF and DM presented in the results is the δ^2H of nonexchangeable H of the organics. However, the DM fraction did not show any significant exchange with surrounding moisture (Supplemental Fig. S2). Dry organic material is likely to be in a temporary hydrophobic state, and thus the exchange is much slower than in the hydrated form (A. Schimmelmann, personal communication; Wassenaar and Hobson, 2000). Moreover, leaf samples were exposed to the same kind of atmospheric moisture, so the exchangeable hydrogen was equilibrated to a common background of water. This

method ensures that relative differences among samples in the DM can be interpreted in terms of parameters that are environmental (i.e. growing conditions) and biological (i.e. biochemical composition of leaf material). Nevertheless, the δ^2H values of the DM presented in the results were also corrected using the fraction of total hydrogen that is exchangeable, obtained within the different equilibration conditions.

In addition, to prove that the extraction water had not influenced the δ^2H of the WSF, further extractions were performed on aliquots of DM from representative samples (the same samples used in the dual-water equilibration method) using four sources of water with different δ^2H: snow water (−77.5‰), deuterated water (+94.4‰), seawater (−3.3‰), and lab water (−43.2‰). Furthermore, the differences between the WSFs were compared. However, using water sources with different δ^2H signatures for extraction did not significantly affect the δ^2H of the soluble fraction; and the absolute differences in δ^2H between soluble fractions extracted from the DM, with the different water sources were minor (Supplemental Table S4). All the measurements were carried out at the Scientific Facilities of the University of Barcelona.

Experimental Estimation of the ETR's Association with δ^2H Depletion

A modern Spanish durum wheat cultivar (Sula) was grown in 3-L pots (three replicates) filled with sand (one plant per pot). Plants were watered three times a week with Hoagland nutrient solution and were grown under controlled conditions in a growth chamber (Conviron E15, Controlled Environments Ltd., Winnipeg, Canada). Plants were supplied with a PPFD of about 400 μM $m^{-2}s^{-1}$ at plant level during the light period (14 h). Plants were grown in a constant RH of 40% or 80% within two different growth chambers, with a temperature of 23°C /17°C during the light and dark periods, respectively. Six flag leaves from the main tiller of different plants grown under different RH (40% or 80%); and the ETR, g_s, and photosynthetic rate of the flag leaf blades were measured using a LI-6400XT portable gas exchange photosynthesis system (Li-COR, Lincoln, NE), approximately 2 weeks after anthesis. The ETR, g_s, and photosynthetic rate were estimated at a saturating PPFD of 1500 μM $m^{-2}s^{-1}$ and 20°C.

Following the ETR measurements, the same six flag leaves from each of the RH conditions, the δ^2H and δ^{13}C in the DM of the leaves, were then analyzed as previously mentioned (see the hydrogen and carbon isotope analysis sections).

In order to support a causal association between the ETR and the effect that ^{2}H-depleted NADPH has on δ^2H of the organic matter, the δ^2H and the ETR in the flag leaf were compared between the different RH treatments (Supplemental Table S1).

Statistical Analysis

Grain yield, agronomic components, and isotopic data were subjected to one-way analyses of variance (ANOVA) using the general linear model to calculate the effects of water regime, N supply, genotype, and their interactions with the studied parameters. Water regime, N supply, and genotype were included as fixed factors, including three blocks and three replicates per block. Means were compared by Tukey's Honest Significant Difference Test and were performed on a combination of water treatments and N supply. Mean values across plant tissues with different letters (*a* and *b*) presented in the tables are significantly different from SI versus RF and HN versus LN, according to Tukey's Honest Significant Difference Test ($P < 0.05$). A bivariate correlation procedure was constructed to analyze the relationships between the measured traits. Statistical analyses were performed using the SPSS 18.0 statistical package (SPSS Inc.). Figures were created using the Sigma-Plot 10.0 program (SPSS Inc.).

SUPPLEMENTAL DATA

The following supplemental materials are available.

Supplemental Figure S1. Polynomial regression between the mean grain yield of the trials and the regression coefficient of the relationship between grain yield carbon, oxygen and hydrogen isotope compositions of different plant components.

Supplemental Figure S2. Mean values of stable isotope composition (‰) of hydrogen (δ^2H) in the water-soluble fraction (WSF) and dry matter (DM) obtained in the dual-water equilibration method.

Supplemental Table S1. Mean values of isotope composition (‰) of hydrogen(δ^2H) and carbon (δ^{13}C) in dry matter and the ETR, g_s, and photosynthetic rate of the flag leaf of plants grown under two different relative humidity conditions in the growth chamber experiment

Supplemental Table S2. Linear regression of the relationship of the carbon (δ^{13}C) oxygen (δ^{18}O) and hydrogen (δ^2H) isotope compositions in the water-soluble fraction (WSF) and dry matter (DM) of the flag leave, ears and mature grains with the grain yield (*GY*)

Supplemental Table S3. Mean values of stable isotope composition (‰) of hydrogen (δ^2H) in the water-soluble fraction (WSF) using four sources of water with different δ^2H for the extraction of the WSF

Supplemental Table S4. Mean values of stable isotope composition (‰) of hydrogen (δ^2H) in the flag leaf water-soluble fraction (WSF) and dry matter (DM) obtained with the dual water equilibration method

ACKNOWLEDGMENTS

Thank you to Kiko Girbés for designing Figure 1. We also thank Arndt Schimmelmann and Ian Begley for their valuable comments on how to quantify the fraction of exchangeable H.

Received February 25, 2019; accepted March 27, 2019; published April 5, 2019.

LITERATURE CITED

Araus JL, Tapia L (1987) Photosynthetic gas exchange characteristics of wheat flag leaf blades and sheaths during grain filling: The case of a spring crop grown under Mediterranean climate conditions. Plant Physiol **85:** 667–673

Araus JL, Brown HR, Febrero A, Bort J, Serret MD (1993) Ear photosynthesis, carbon isotope discrimination and the contribution of respiratory CO_2 to differences in grain mass in durum wheat. Plant Cell Environ **16:** 383–392

Araus JL, Amaro T, Casadesús J, Asbati A, Nachit MM (1998) Relationships between ash content, carbon isotope discrimination and yield in durum wheat. Aust J Plant Physiol **25:** 835–842

Araus JL, Slafer GA, Reynolds MP, Royo C (2002) Plant breeding and drought in C_3 cereals: What should we breed for? Ann Bot **89:** 925–940

Araus JL, Villegas D, Aparicio N, García del Moral LF, El Hani S, Rharrabti Y, Ferrio JP, Royo C (2003) Environmental factors determining carbon isotope discrimination and yield in durum wheat under Mediterranean conditions. Crop Sci **43:** 170–180

Araus JL, Ferrio JP, Buxó R, Voltas J (2007) The historical perspective of dryland agriculture: Lessons learned from 10,000 years of wheat cultivation. J Exp Bot **58:** 131–145

Araus JL, Cabrera-Bosquet L, Serret MD, Bort J, Nieto-Taladriz MT (2013) Comparative performance of δ^{13}C, δ^{18}O and δ^{15}N for phenotyping durum wheat adaptation to a dryland environment. Funct Plant Biol **40:** 595–608

Barbour MM (2007) Stable oxygen isotope composition of plant tissue: A review. Funct Plant Biol **34:** 83–94

Barbour MM, Farquhar GD (2000) Relative humidity- and ABA-induced variation in carbon and oxygen isotope ratios of cotton leaves. Plant Cell Environ **23:** 473–485

Barbour MM, Fischer RA, Sayre KD, Farquhar GD (2000) Oxygen isotope ratio of leaf and grain material correlates with stomatal conductance and grain yield in irrigated wheat. Aust J Plant Physiol **27:** 625–637

Barbour MM, Roden JS, Farquhar GD, Ehleringer JR (2004) Expressing leaf water and cellulose oxygen isotope ratios as enrichment above source water reveals evidence of a Péclet effect. Oecologia **138:** 426–435

Barlow EWR, Lee JW, Munns R, Smart MG (1980) Water relations of the developing wheat grain. Aust J Plant Physiol **7:** 519

Bloom AJ (2015) Photorespiration and nitrate assimilation: A major intersection between plant carbon and nitrogen. Photosynth Res **123:** 117–128

Blum A (1985) Photosynthesis and transpiration in leaves and ears of wheat and barley varieties. J Exp Bot **36:** 432–440

Bort J, Febrero A, Amaro T, Araus J (1994) Role of awns in ear water-use efficiency and grain weight in barley. Agronomie **14:** 133–139

Bort J, Brown RH, Araus JL (1996) Refixation of respiratory CO_2 in the ears of C_3 cereals. J Exp Bot **47:** 1567–1575

Bottinga Y, Craig H (1968) Oxygen isotope fractionation between CO_2 and water, and the isotopic composition of marine atmospheric CO_2. Earth Planet Sci Lett **5:** 285–295

Buchanan BB, Gruissem W, Jones RL editors (2015) Biochemistry & Molecular Biology of Plants, Ed 2. Wiley Blackwell, Oxford UK

Cabrera-Bosquet L, Molero G, Nogués S, Araus JL (2009a) Water and nitrogen conditions affect the relationships of $\Delta^{13}C$ and $\Delta^{18}O$ to gas exchange and growth in durum wheat. J Exp Bot **60:** 1633–1644

Cabrera-Bosquet L, Sánchez C, Araus JL (2009b) Oxygen isotope enrichment ($\Delta^{18}O$) reflects yield potential and drought resistance in maize. Plant Cell Environ **32:** 1487–1499

Cabrera-Bosquet L, Albrizio R, Nogués S, Araus JL (2011) Dual $\Delta^{13}C/\delta^{18}O$ response to water and nitrogen availability and its relationship with yield in field-grown durum wheat. Plant Cell Environ **34:** 418–433

Caley CY, Duffus CM, Jeffcoat B (1990) Photosynthesis in the pericarp of developing wheat grains. J Exp Bot **41:** 303–307

Ceglar A, Toreti A, Lecerf R, Van der Velde M, Dentener F (2016) Impact of meteorological drivers on regional inter-annual crop yield variability in France. Agricultural and Forest Meteorol **216:** 58–67

Cernusak LA, Farquhar GD, Pate JS (2005) Environmental and physiological controls over oxygen and carbon isotope composition of Tasmanian blue gum, *Eucalyptus globulus*. Tree Physiol **25:** 129–146

Cernusak LA, Winter K, Aranda J, Turner BL, Marshall JD (2007) Transpiration efficiency of a tropical pioneer tree (*Ficus insipida*) in relation to soil fertility. J Exp Bot **58:** 3549–3566

Cernusak LA, Mejia-Chang M, Winter K, Griffiths H (2008) Oxygen isotope composition of CAM and C_3*Clusia* species: Non-steady-state dynamics control leaf water ^{18}O enrichment in succulent leaves. Plant Cell Environ **31:** 1644–1662

Cernusak LA, Barbour MM, Arndt SK, Cheesman AW, English NB, Feild TS, Helliker BR, Holloway-Phillips MM, Holtum JAM, Kahmen A, et al (2016) Stable isotopes in leaf water of terrestrial plants. Plant Cell Environ **39:** 1087–1102

Chikaraishi Y, Naraoka H (2003) Compound-specific δD–$\delta^{13}C$ analyses of *n*-alkanes extracted from terrestrial and aquatic plants. Phytochemistry **63:** 361–371

Chikaraishi Y, Naraoka H, Poulson SR (2004) Carbon and hydrogen isotopic fractionation during lipid biosynthesis in a higher plant (*Cryptomeria japonica*). Phytochemistry **65:** 323–330

Cochrane MP, Duffus CM (1979) Morphology and ultrastructure of immature cereal grains in relation to transport. Ann Bot **44:** 67–72

Condon AG, Richards RA, Farquhar GD (1987) Carbon isotope discrimination is positively correlated with grain yield and dry matter production in field-grown wheat. Crop Sci **27:** 996–1001

Condon AG, Richards RA, Rebetzke GJ, Farquhar GD (2004) Breeding for high water-use efficiency. J Exp Bot **55:** 2447–2460

Coplen TB (1988) Normalization of oxygen and hydrogen isotope data. Chem Geol (Isot Geosci Sect) **72:** 293–297

Cormier M-A, Werner RA, Sauer PE, Gröcke DR, Leuenberger MC, Wieloch T, Schleucher J, Kahmen A (2018) ^2H-fractionations during the biosynthesis of carbohydrates and lipids imprint a metabolic signal on the δ^2H values of plant organic compounds. New Phytol **218:** 479–491

Craig H, Gordon LI (1965) Deuterium and oxygen-18 variations in the ocean and the marine atmosphere. In Tongiorgi, ed., Proceedings of a Conference on Stable Isotopes in Oceanographic Studies and Paleotemperatures, Lischi and Figli, Pisa, pp. 9–130

Cuntz M, Ogée J, Farquhar GD, Peylin P, Cernusak LA (2007) Modelling advection and diffusion of water isotopologues in leaves. Plant Cell Environ **30:** 892–909

Dansgaard W (1964) Stable isotopes in precipitation. Tellus **16:** 436–468

Dawson TE, Ehleringer JR (1993) Isotopic enrichment of water in the "woody" tissues of plants: Implications for plant water source, water uptake, and other studies which use the stable isotopic composition of cellulose. Geochim Cosmochim Acta **57:** 3487–3492

Dawson TE, Mambelli S, Plamboeck AH, Templer PH, Tu KP (2002) Stable isotopes in plant ecology. Annu Rev Ecol Syst **33:** 507–559

Epstein S, Yapp CJ, Hall JH (1976) The determination of the D/H ratio of non-exchangeable hydrogen in cellulose extracted from aquatic and land plants. Earth Planet Sci Lett **30:** 241–251

Epstein S, Thompson P, Yapp CJ (1977) Oxygen and hydrogen isotopic ratios in plant cellulose. Science **198:** 1209–1215

Farquhar GD, Gan KS (2003) On the progressive enrichment of the oxygen isotopic composition of water along a leaf . Plant Cell Environ **26:** 1579–1597

Farquhar GD, Lloyd J (1993) Carbon and oxygen isotope effects in the exchange of carbon dioxide between terrestrial plants and the atmosphere. In A Ehleringer, J Hall, G Farquhar, eds, Stable Isotopes and Plant Carbon–Water Relations, Academic P., San Diego, pp 47–70

Farquhar G, Richards RA (1984) Isotopic composition of plant carbon correlates with water-use efficiency of wheat genotypes. Aust J Plant Physiol **11:** 539–552

Farquhar GD, Oleary MH, Berry JA (1982) On the relationship between carbon isotope discrimination and the intercellular carbon dioxide concentration in leaves. Aust J Plant Physiol **9:** 121–137

Farquhar G, Ehleringer JR, Hubick KT (1989) Carbon isotope discrimination and photosynthesis. Annu Rev Plant Physiol Plant Mol Biol **40:** 503–537

Farquhar G, Barbour MM, Henry BK (1998) Interpretation of oxygen isotope composition of leaf material. In.HG Griffiths, ed, Stable Isotopes: Integration of Biochemical, Ecological and Geochemical Processes, Bios Scien, Oxford, pp 27–62

Farquhar GD, Cernusak LA, Barnes B (2007) Heavy water fractionation during transpiration. Plant Physiol **143:** 11–18

Feakins SJ, Sessions AL (2010) Controls on the D/H ratios of plant leaf waxes in an arid ecosystem. Geochim Cosmochim Acta **74:** 2128–2141

Ferrio JP, Mateo MA, Bort J, Abdalla O, Voltas J, Araus JL (2007) Relationships of grain $\delta^{13}C$ and $\delta^{18}O$ with wheat phenology and yield under water-limited conditions. Ann Appl Biol **150:** 207–215

Filot MS, Leuenberger M, Pazdur A, Boettger T (2006) Rapid online equilibration method to determine the D/H ratios of non-exchangeable hydrogen in cellulose. Rapid Commun Mass Spectrom **20:** 3337–3344

Fischer RA, Rees D, Sayre KD, Lu Z-M, Condon AG, Larqué-Saavedra A (1998) Wheat yield progress associated with higher stomatal conductance and photosynthetic rate, and cooler canopies. Crop Sci **38:** 1467–1475

Flanagan C, Comstock JP, Ehleringer JR (1991) Comparison of modeled and observed environmental influences on the stable oxygen and hydrogen isotope composition of leaf water in *Phaseolus vulgaris* L. Plant Physiol **96:** 588–596

Food and Agriculture Organization of the United Nations (FAOSTAT) (2017) http://www.fao.org/home/en/ (July 25, 2017)

Foyer CH, Neukermans J, Queval G, Noctor G, Harbinson J (2012) Photosynthetic control of electron transport and the regulation of gene expression. J Exp Bot **63:** 1637–1661

Gessler A, Ferrio JP, Hommel R, Treydte K, Werner RA, Monson RK (2014) Stable isotopes in tree rings: Towards a mechanistic understanding of isotope fractionation and mixing processes from the leaves to the wood. Tree Physiol **34:** 796–818

Gonfiantini R (1978) Standards for stable isotope measurements in natural compounds. Nature **271:** 534–536

Gonfiantini R, Gratziu S, Tongiorgi E (1965) Oxygen isotopic composition of water in leaves. Symposium of the Use of Isotopes and Radiation in Soil-Plant Nutrition Studies, International Atomic Energy Agency, Vienna, pp 405–410

Hayes JM (2001) Fractionation of carbon and hydrogen isotopes in biosynthetic processes. Rev Mineral Geochem **43:** 225–277

Helliker BR, Ehleringer JR (2000) Establishing a grassland signature in veins: ^{18}O in the leaf water of C_3 and C_4 grasses. Proc Natl Acad Sci USA **97:** 7894–7898

Helliker BR, Ehleringer JR (2002) Differential ^{18}O enrichment of leaf cellulose in C_3 *versus* C_4 grasses. Funct Plant Biol **29:** 435–442

Hoganson CW, Babcock GT (1997) A metalloradical mechanism for the generation of oxygen from water in photosynthesis. Science **277:** 1953–1956

Hou J, D'Andrea WJ, MacDonald D, Huang Y (2007) Hydrogen isotopic variability in leaf waxes among terrestrial and aquatic plants around Blood Pond, Massachusetts (USA). Org Geochem **38:** 977–984

Hubick KT, Hammer GL, Farquhar GD, Wade LJ, von Caemmerer S, Henderson SA (1990) Carbon isotope discrimination varies genetically in c_4 species. Plant Physiol **92:** 534–537

Jensen A, Lorenzen B, Østergaard HS, Hvelplund EK (1990) Radiometric estimation of biomass and nitrogen content of barley grown at different nitrogen levels. Int J Remote Sens **11:** 1809–1820

Jia S, Lv J, Jiang S, Liang T, Liu C, Jing Z (2015) Response of wheat ear photosynthesis and photosynthate carbon distribution to water deficit. Photosynthetica **53:** 95–109

Kahmen A, Schefuß E, Sachse D (2013) Leaf water deuterium enrichment shapes leaf wax *n*-alkane δD values of angiosperm plants I: Experimental evidence and mechanistic insights. Geochim Cosmochim Acta **111:** 39–49

Knoppik D, Selinger H, Ziegler-Jöns A (1986) Differences between the flag leaf and the ear of a spring wheat cultivar (*Triticum aestivum* cv. Arkas) with respect to the CO_2 response of assimilation, respiration and stomatal conductance. Physiol Plant **68:** 451–457

Li X, Wang H, Li H, Zhang L, Teng N, Lin Q, Wang J, Kuang T, Li Z, Li B, et al (2006) Awns play a dominant role in carbohydrate production during the grain-filling stages in wheat (*Triticum aestivum*). Physiol Plant **127:** 701–709

Liu H, Guo B, Wei Y, Wei S, Ma Y, Zhang W (2015) Effects of region, genotype, harvest year and their interactions on δ^{13}C, δ^{15}N and δD in wheat kernels. Food Chem **171:** 56–61

Lobell DB, Burke MB, Tebaldi C, Mastrandrea MD, Falcon WP, Naylor RL (2008) Prioritizing climate change adaptation needs for food security in 2030. Science **319:** 607–610

Lopes MS, Reynolds MP (2010) Dissecting drought adaptation into its phenotypic and genetic components in wheat. Asp Appl Biol 105: 7–11

Luo Y, Sternberg L (1991) Deuterium heterogeneity in starch and cellulose nitrate of cam and C_3 plants. Phytochemistry **30:** 1095–1098

Luo Y-H, Steinberg L, Suda S, Kumazawa S, Mitsui A (1991) Extremely low D/H ratios of photoproduced hydrogen by cyanobacteria. Plant Cell Physiol **32:** 897–900

Martín-Gómez P, Barbeta A, Voltas J, Peñuelas J, Dennis K, Palacio S, Dawson TE, Ferrio JP (2015) Isotope-ratio infrared spectroscopy: A reliable tool for the investigation of plant-water sources? New Phytol **207:** 914–927

Monneveux P, Reynolds MP, Trethowan R, González-Santoyo H, Peña RJ, Zapata F (2005) Relationship between grain yield and carbon isotope discrimination in bread wheat under four water regimes. Eur J Agron **22:** 231–242

Moore FC, Lobell DB (2015) The fingerprint of climate trends on European crop yields. Proc Natl Acad Sci USA **112:** 2670–2675

Offermann C, Ferrio JP, Holst J, Grote R, Siegwolf R, Kayler Z, Gessler A (2011) The long way down—Are carbon and oxygen isotope signals in the tree ring uncoupled from canopy physiological processes? Tree Physiol **31:** 1088–1102

Oweis T, Pala M, Ryan J (1998) Stabilizing rainfed wheat yields with supplemental irrigation and nitrogen in a Mediterranean climate. Agron J **90:** 672–681

Pande PC, Datta PS, Bhattacharya SK (1994) Biphasic enrichment of $H_2{}^{18}O$ in developing wheat grain water. Indian J Plant Physiol **37:** 30–31

Pande PC, Datta PS, Bhattacharya SK, Tyagi SK (1995) Post-anthesis metabolic-enrichment of $H_2{}^{18}O$ in wheat grain. Indian J Exp Biol **33:** 394–396

Qi H, Coplen TB (2011) Investigation of preparation techniques for δ^2H analysis of keratin materials and a proposed analytical protocol. Rapid Commun Mass Spectrom **25:** 2209–2222

Richards RA (1996) Defining selection criteria to improve yield under drought. Plant Growth Regul **20:** 157–166

Richards RA, Rebetzke GJ, Condon AG, van Herwaarden AF (2002) Breeding opportunities for increasing the efficiency of water use and crop yield in temperate cereals. Crop Sci **42:** 111–121

Rieder SV, Rose IA (1959) The mechanism of the triosephosphate isomerase reaction. J Biol Chem **234:** 1007–1010

Roden JS, Lin G, Ehleringer JR (2000) A mechanistic model for interpretation of hydrogen and oxygen isotope ratios in tree-ring cellulose. Geochim Cosmochim Acta **64:** 21–35

Sachse D, Radke J, Gleixner G (2006) δD values of individual *n*-alkanes from terrestrial plants along a climatic gradient—Implications for the sedimentary biomarker record. Org Geochem **37:** 469–483

Sachse D, Billault I, Bowen GJ, Chikaraishi Y, Dawson TE, Feakins SJ, Freeman KH, Magill CR, McInerney FA, Van der Meer MTJ, et al (2012) Molecular paleohydrology: Interpreting the hydrogen-isotopic composition of lipid biomarkers from photosynthesizing organisms. Annu Rev Earth Planet Sci **40:** 221–249

Sadras VO (2004) Yield and water-use efficiency of water- and nitrogen-stressed wheat crops increase with degree of co-limitation. Eur J Agron **21:** 455–464

Salazar-Tortosa D, Castro J, Villar-Salvador P, Viñegla B, Matías L, Michelsen A, Rubio de Casas R, Querejeta, JI (2018) The "isohydric trap": A proposed feedback between water shortage, stomatal regulation, and nutrient acquisition drives differential growth and survival of European pines under climatic dryness. Glob Chang Biol **24:** 4069–4083

Sanchez-Bragado R, Elazab A, Zhou B, Serret MD, Bort J, Nieto-Taladriz MT, Araus JL (2014) Contribution of the ear and the flag leaf to grain filling in durum wheat inferred from the carbon isotope signature: Genotypic and growing conditions effects. J Integr Plant Biol **56:** 444–454

Sánchez-Bragado R, Araus JL, Scheerer U, Cairns JE, Rennenberg H, Ferrio JP (2016) Factors preventing the performance of oxygen isotope ratios as indicators of grain yield in maize. Planta **243:** 355–368

Sauer PE, Schimmelmann A, Sessions AL, Topalov K (2009) Simplified batch equilibration for D/H determination of non-exchangeable hydrogen in solid organic material. Rapid Commun Mass Spectrom **23:** 949–956

Schimmelmann A (1991) Determination of the concentration and stable isotopic composition of nonexchangeable hydrogen in organic matter. Anal Chem **63:** 2456–2459

Schimmelmann A, Lawrence M, Michael E (2001) Stable isotopes ratios of organic H, C and N in the Miocene Monterey Formation, California. In CM Isaac, J Rullkötter, eds, Monterey Formation: From Rocks to Molecules, Columbia University Press, New York, pp 86–106

Schleucher J, Vanderveer P, Markley JL, Sharkey TD (1999) Intramolecular deuterium distributions reveal disequilibrium of chloroplast phosphoglucose isomerase. Plant Cell Environ **22:** 525–533

Schmidt HL, Werner RA, Eisenreich W (2003) Systematics of ^{2}H patterns in natural compounds and its importance for the elucidation of biosynthetic pathways. Phytochem Rev **2:** 61–85

Schmidt HL, Robins RJ, Werner RA (2015) Multi-factorial in vivo stable isotope fractionation: Causes, correlations, consequences and applications. Isotopes Environ Health Stud **51:** 155–199

Schwendenmann L, Pendall E, Sanchez-Bragado R, Kunert N, Hölscher D (2015) Tree water uptake in a tropical plantation varying in tree diversity: Interspecific differences, seasonal shifts and complementarity. Ecohydrology **8:** 1–12

Serret MD, Ortiz-Monasterio I, Pardo A, Araus JL (2008) The effects of urea fertilisation and genotype on yield, nitrogen use efficiency, δ^{15}N and δ^{13}C in wheat. Ann Appl Biol **153:** 243–257

Sessions AL, Burgoyne TW, Schimmelmann A, Hayes JM (1999) Fractionation of hydrogen isotopes in lipid biosynthesis. Org Geochem **30:** 1193–1200

Shangguan ZP, Shao MA, Dyckmans J (2000) Nitrogen nutrition and water stress effects on leaf photosynthetic gas exchange and water use efficiency in winter wheat. Environ Exp Bot **44:** 141–149

Smith FA, Freeman KH (2006) Influence of physiology and climate on δD of leaf wax *n*-alkanes from C_3 and C_4 grasses. Geochim Cosmochim Acta **70:** 1172–118

Song X, Farquhar GD, Gessler A, Barbour MM (2014) Turnover time of the non-structural carbohydrate pool influences δ^{18}O of leaf cellulose. Plant Cell Environ **37:** 2500–2507

Sternberg L (1988) D/H ratios of environmental water recorded by D/H ratios of plant lipids. Nature **333:** 59–61

Sternberg L, Deniro MJ (1983) Isotopic composition of cellulose from C_3, C_4, and CAM plants growing near one another. Science **220:** 947–949

Sternberg LO, Deniro MJ, Johnson HB (1984) Isotope ratios of cellulose from plants having different photosynthetic pathways. Plant Physiol **74:** 557–561

Sternberg LdaS, Deniro MJ, Savidge RA (1986) Oxygen isotope exchange between metabolites and water during biochemical reactions leading to cellulose synthesis. Plant Physiol **82:** 423–427

Tambussi EA, Nogués S, Araus JL (2005) Ear of durum wheat under water stress: Water relations and photosynthetic metabolism. Planta **221:** 446–458

Voltas J, Romagosa I, Lafarga A, Armesto AP, Araus JL, Sombrero A (1999) Genotype by environment interaction for grain yield and carbon isotope discrimination of barley in Mediterranean Spain. Aust J Agric Res **50:** 1263–1271

Wassenaar LI, Hobson KA (2000) Improved method for determining the stable-hydrogen isotopic composition (δmproved method for determining the stable-hydrogen isotop. Envirn. Sci. Technol. **34:** 2354–2360.

Williams DG, Coltrain JB, Lott M, English NB, Ehleringer JR (2005) Oxygen isotopes in cellulose identify source water for archaeological maize in the American Southwest. J Archaeol Sci **32:** 931–939

Winter K, Holtum JAM (2014) Facultative crassulacean acid metabolism (CAM) plants: Powerful tools for unravelling the functional elements of CAM photosynthesis. J Exp Bot **65:** 3425–3441

Winter K, Garcia M, Holtum JAM (2008) On the nature of facultative and constitutive CAM: Environmental and developmental control of CAM expression during early growth of Clusia, Kalanchöe, and Opuntia. J Exp Bot **59:** 1829–1840

Yakir D (1992) Variations in the natural abundance of oxygen-18 and deuterium in plant carbohydrates. Plant Cell Environ **15:** 1005–1020

Yakir D, Deniro MJ (1990) Oxygen and hydrogen isotope fractionation during cellulose metabolism in *Lemna gibba* L. Plant Physiol **93:** 325–332

Yakir D, Deniro MJ, Ephrath JE (1990a) Effects of water stress on oxygen, hydrogen and carbon isotope ratios in two species of cotton plants. Plant Cell Environ **13:** 949–955

Yakir D, Deniro MJ, Gat JR (1990b) Natural deuterium and oxygen-18 enrichment in leaf water of cotton plants grown under wet and dry conditions: Evidence for water compartmentation and its dynamics. Plant Cell Environ **13:** 49–56

Yang H, Leng Q (2009) Molecular hydrogen isotope analysis of living and fossil plants—*Metasequoia* as an example. Prog Nat Sci **19:** 901–912

Yousfi S, Serret MD, Araus JL (2013) Comparative response of $\delta^{13}C$, $\delta^{18}O$ and $\delta^{15}N$ in durum wheat exposed to salinity at the vegetative and reproductive stages. Plant Cell Environ **36:** 1214–1227

Zadoks JC, Chang TT, Konzak CF (1974) A decimal code for the growth stages of cereals. Weed Res **14:** 415–421

Zhao LJ, Xiao HL, Liu XH (2007) Relationships between carbon isotope discrimination and yield of spring wheat under different water and nitrogen levels. J Plant Nutr **30:** 947–963

Zhou Y, Stuart-Williams H, Farquhar GD, Hocart CH (2010) The use of natural abundance stable isotopic ratios to indicate the presence of oxygen-containing chemical linkages between cellulose and lignin in plant cell walls. Phytochemistry **71:** 982–993

Zhou Y, Grice K, Chikaraishi Y, Stuart-Williams H, Farquhar GD, Ohkouchi N (2011) Temperature effect on leaf water deuterium enrichment and isotopic fractionation during leaf lipid biosynthesis: Results from controlled growth of C_3 and C_4 land plants. Phytochemistry **72:** 207–213

Zhou Y, Zhang B, Stuart-Williams H, Grice K, Hocart CH, Gessler A, Kayler ZE, Farquhar GD (2018) On the contributions of photorespiration and compartmentation to the contrasting intramolecular ^2H profiles of C_3 and C_4 plant sugars. Phytochemistry **145:** 197–206

Ziegler H (1989) Hydrogen isotope fractionation in plant tissues. *In* Stable Isotopes in Ecological Research. In P Rundel, JR Ehleringer, K Nagy, eds, Springer-Verlag, New York, pp 105–123

Ziegler H, Osmond CB, Stichler W, Trimborn P (1976) Hydrogen isotope discrimination in higher plants: Correlations with photosynthetic pathway and environment. Planta **128:** 85–92